August 2013

Development of Green Solvent Modified Zeolite (gsmz) for the Removal of Chemical Contaminants from Water

Elizabeth Stapleton
University of Wisconsin-Milwaukee

DEVELOPMENT OF GREEN SOLVENT MODIFIED ZEOLITE (GSMZ) FOR THE REMOVAL OF CHEMICAL CONTAMINANTS FROM WATER

by

Elizabeth R. Stapleton

A Thesis Submitted in

Partial Fulfillment of the

Requirements for the Degree of

Master of Science

in Geosciences

at

The University of Wisconsin-Milwaukee

August 2013

DEVELOPMENT OF GREEN SOLVENT MODIFIED ZEOLITE (GSMZ) FOR THE REMOVAL OF CHEMICAL CONTAMINANTS FROM WATER

by

Elizabeth R. Stapleton

The University of Wisconsin-Milwaukee, 2013
Under the Supervision of Shangping Xu, Ph.D.

Sorption represents an important strategy in the remediation of groundwater contamination. As a naturally-occurring mineral with large cation exchange capacity, zeolite is negatively charged and has been widely used as an inexpensive and effective sorbent for the removal of positively charged contaminants. The negative charges of zeolite, however, make it generally ineffective in the sorption of anionic contaminants such as chromate Cr(VI) and arsenate As(V). In order to improve the capacity for sorption of anionic species, the surface charge of the zeolite must be modified. Cationic surfactants can be used to alter the surface charge of the minerals so that the negatively charged heavy metals can be removed.

The adsorption equilibrium and kinetics data for adsorption of As(V) and Cr(VI) from an aqueous solution onto a green solvent modified zeolite (GSMZ) were determined through batch experiments. A natural zeolite from St. Cloud New Mexico was modified by the surfactant HDmim, from the imidazolium group of chemicals, which are considered as “green solvents”. The effects of ionic strength and solution pH on the sorption capacity of As(V) and Cr(VI) on GSMZ were evaluated. Our results indicate that pH has little effect on the removal of both As(V) and Cr(VI) on GSMZ. Zeta potential tests show that for the pH range tested (4-9) the surface charge of the modified

zeolite is consistently positive. The removal of arsenate and chromate by GSMZ does not appear to be dependent on speciation at different pH. Meanwhile, competition by chloride ions at different ionic strength was found to have an impact on sorption capacity. The Langmuir competition model was applied to experimental adsorption data to determine the extent of competition between the heavy metal ions and chloride anions. Compared to results from previously modified zeolites, GSMZ performed well, with a sorption maximum for chromate of about 26 mM/kg and a sorption maximum for arsenate of about 12 mM./kg.

TABLE OF CONTENTS

LIST OF FIGURES

LIST OF TABLES

LIST OF SYMBOLS

S	Amount of heavy metal sorbed on the solid surfaces at equilibrium (mM/kg)
K_{As}	Langmuir coefficient for arsenate (L/mM)
K_{Cl}	Langmuir coefficient for chloride (L/mM)
K_{Cr}	Langmuir coefficient for chromate (L/mM)
S_m	Sorption capacity/maximum (mM/kg)
C	Equilibrium heavy metal liquid concentration (mM/L)
Cr(III)	chromite
Cr(VI)	chromate
As(III)	arsenite
As(VI)	arsenate
SMZ	Surfactant Modified Zeolite
GSMZ	Green Solvent Modified Zeolite
HDTMA	hexadecyltrimethylammonium
HDmim	1-hexadecyl-3-methylimidazolium
AAS	Atomic Adsorption Spectrophotometry
CMC	Critical micelle concentration
ECEC	External cation exchange capacity

ACKNOWLEDGMENTS

This research was supported by University of Wisconsin-Milwaukee, the University of Wisconsin-Milwaukee Research Foundation, and the Wisconsin Geological Society. I would like to thank the members of my defense committee for their consideration and input toward my thesis: Dr. Shangping Xu, Dr. Timothy Grundl, and Dr. Weon Shik Han. I would also like to thank my parents for their support in the pursuing of my Master's degree and also for the love and support they have shown me throughout my entire educational career.

1. INTRODUCTION

Naturally-occurring heavy metals and metalloids can be released into groundwater sources by mining, natural dissolution, and industrial processing (Terlecka, 2005; Leyva-Ramos et al, 2008). Arsenic and chromium are number 1 and 17 respectively on a list of 275 most commonly found groundwater contaminants at Superfund sites in the United States (Agency for Toxic Substances and Disease Registry, 2011). Contamination by arsenic and chromium poses a potential health threat, as both species are considered carcinogenic to humans (Burke et al, 1991; Sharma et al, 2012; Terlecka, 2005). Recently, outbreaks of cancer and dermatitis in countries including India, Bangladesh, Vietnam, and Japan have brought more attention to the issue of heavy metals in drinking water and the importance of finding practical and cost-effective means of removing these negatively charged species (Berg et al, 2001; Chowdhury et al, 2000; Sharma et al, 2012; Tokyo Metropolitan Government Bureau of Sanitation, 1987; Smith, Lingas, and Rahman, 2000). Different methods for chromate and arsenate removal have been tested including sorption by zero-valent iron, activated carbon, synthesized nano-materials, and modified zeolites (Biterna, et al, 2007; Farrell et al, 2001; Melitas et al, 2002; Liu et al, 2010; Hristovski et al, 2008; Ponder et al. 2000, Shi et al. 2011; Bautistatoledo et al. 1994; Chowdhury and Yanful 2010, Sharma et al. 2010; Li et al., 1998). In the past 20 years, modified zeolites have gained popularity for their use in contamination removal and one type of modified zeolite, HDTMA-modified zeolite, has recently (2007) been patented and marketed for use in water treatment (Schulze-Makuch, Bowman, and Pillai, 2003; Bowman, 2005; Li et al, 1998).

2. LITERATURE REVIEW

2.1 Zeolite

Zeolites are naturally-occurring minerals known for being effective molecular sieves and for having high cation exchange capacities (Davis and Lobo, 1992; St. Cloud Mining, 2012). Natural zeolites can be mined primarily from volcanic rocks such as volcanic tuff (St. Cloud Mining, 2012). There are over 40 different minerals classified as zeolites and each has a slightly different structure (Georgiev, 2009). Zeolites are aluminosilicate minerals which are constructed of a three-dimensional network of $[SiO^4]^{4-}$ and $[AlO^4]^{5-}$ tetrahedra which are linked together by sharing oxygen atoms (Breck, 1974). Because of this three-dimensional structure, zeolites are porous and consist of a series of interconnected channels (Breck, 1974; Georgiev, 2009). These channels give the zeolites a function as a molecular sieve, whereby particles larger than a certain size (typically 0.3 to 0.7 nm in diameter) will be removed from a solution, so that it can be used to selectively screen molecules based on size (Davis and Lobo, 1992; St. Cloud Mining, 2012). These pores also allow for excellent cation exchange properties.

Zeolites are a promising material for contaminant remediation. Like clay minerals, zeolites have a high cationic exchange capacity, which is ideal for the removal of cationic contaminants such as mercury or cobalt. Unlike smectite clays, zeolites have a rigid three-dimensional structure and have more ideal hydraulic properties (Georgiev, 2009). For example, the estimated hydraulic conductivity of compacted zeolite is about 2×10^{-5}, while clays typically have hydraulic conductivities of about 1×10^{-10} (Oren and Ozdamar, 2013; Benson and Trast, 1995). The higher hydraulic conductivity values of zeolites as compared to clays suggest that the material will allow higher volumes of

contaminated water to travel through a permeable barrier in less time. These properties are necessary for the construction of a permeable barrier.

As a naturally-occurring mineral with large cation exchange capacity, zeolite is negatively charged and has been widely used as an inexpensive and yet effective sorbent for the removal of positively charged contaminants such as heavy metals from water (Rasouli et al. 2012, Salem et al. 2012, Schick et al. 2012, Shinzato et al. 2012). The negative charges of zeolite, however, make it ineffective in the sorption of anionic contaminants such as chromate or arsenate.

2.2 Surfactant Modification of Natural Zeolite

Attempts were made to use surfactants to modify the surface of zeolite and the thus produced surfactant modified zeolite was found to be suitable for the removal of anionic contaminants (Li 1998, Li et al. 1998, Li and Bowman 1998, Li et al. 2000, Li and Bowman 2001). Cationic surfactants can be applied to the natural zeolite in order to alter the surface charge to positive. When the concentration of the cationic surfactant is higher than its critical micelle concentration (CMC), the sorbed surfactant molecules on zeolite form bilayers (Li, Anghel, and Bowman, 1998). The initial monolayer is created by cationic exchange at the surface of the zeolite, while the bilayer is formed through hydrophobic interactions (Li and Bowman, 1998; Leyva-Ramos et al, 2008). The bilayer is stabilized at equilibrium by counterions. The creation of a stable bilayer gives the zeolite anionic exchange capabilities.

Different types of cationic surfactants are available and have been tested on zeolite. Most commonly used in the past was the surfactant hexadecyltrimethylammonium (HDTMA). This surfactant has been well-tested and

characterized by Li and Bowman (1998) and has been used by many others in a wide range of applications. Such applications include removal of organic compounds from oilfield water, removal of pathogens from both wastewater and groundwater, and chemical contaminant removal (Ranck et al, 2005; Schulze-Makuch, 2003; Bowman, 2003; Li, 2007).

Unlike sufactants commonly employed in zeolite surface manipulation such as HDTMA, the surfactant HDmim, which belongs to the imadizolium group of green solvents, is more stable and is considered as more environmentally friendly.

2.3 Chromium

The heavy metal chromium is a naturally occurring element which can be toxic. Chromium can be directly mined and introduced into the environment. Large quantities of chromium were released into the natural environment as a result of the processing of the ores for chromium production and its industrial applications (Xu and Jaffe 2006). For instance, it was estimated that more than 72 million kilograms of chromium was released at ~110 sites that were used to process chromite ores within the United States (Palmer and Wittbrodt, 1991). Furthermore, chromium is utilized in various industries such as metallurgy (e.g., stainless steel and plating), leather tanning, wood preservation, dye and pigment production and petroleum processing (Nriagu and Nieboer, 1988; Kotas and Stasicka, 2000). It is by these processes that contamination by chromium typically enters the natural environment and contaminates soil and groundwater.

In the natural environment, the oxidation number of chromium can vary between 0 and 6 and the most stable ionic forms of chromium include Cr(III) and Cr(VI) (Fruchter, 2002). In general, Cr(VI) is toxic, has high solubility in water, and tends to display high

mobility within the soil-groundwater system. In contrast, Cr(III) has low solubility and is considered as a necessary micro-nutrient for living organisms at low concentrations (California EPA, 2011). The remediation of Cr(VI) contamination in soil and groundwater thus often involves the adsorption and immobilization of Cr(VI) using high-capacity adsorbents and/or the reduction of Cr(VI) to Cr(III) which tends to form precipitates (e.g., $Cr(OH)_3$) under ambient pH conditions.

The environmental behavior of Cr(VI) is determined by its speciation, which in turn depends on pH and its total concentration (Tandon et al., 1984, Kotas and Stasicka, 2000). H_2CrO_4 tends to deprotonate when the pH is higher than 1. When pH is between 1 and 7, $HCrO_4^-$ represents the most abundant Cr(VI) species. Under basic pH conditions (i.e., pH>7), Cr(VI) mainly exists as CrO_4^{2-} (Tandon et al. 1984, Kotas and Stasicka 2000). Additionally, when pH is within 1 to 6 and the total Cr(VI) concentration is higher than 10^{-2} M, the condensation of $HCrO_4^-$ can lead to the formation of $Cr_2O_7^{2-}$ (Cotton, 1999; Kotas and Stasicka, 2000).

The sorbents that have been developed and tested for Cr(VI) removal and immobilization include natural or surface modified clays (Li 1998, Li et al. 2007, Leyva-Ramos et al. 2008), metal oxide/hydroxide (Mohan and Pittman 2006), iron containing minerals and zero-valent iron (Blowes et al. 1997, Ponder et al. 2000, Shi et al. 2011), activated carbon (Bautistatoledo et al. 1994), biosorbent (Hou et al. 2012), iron (III)-doped biopolymer gels (Min and Hering 1999), as well as synthesized nano materials (Chowdhury and Yanful 2010, Sharma et al. 2010, Zhao et al. 2010, Dhiwar et al. 2011, Li et al. 2012). For the *in-situ* remediation of groundwater Cr(VI) contamination where large quantities of the sorbents are generally needed, the sorbents that display high

capacity and have low cost are preferred.

2.4 Arsenic

Arsenic is considered to be one of the most toxic pollutants and causes carcinogenic and mutagenic effects in humans (Mendoza-Barron et al, 2010; Terlecka, 2005). Arsenic can enter the natural environment by dissolution of minerals from weathered rocks and soils, meteoric leaching of mine wastes, and use of agricultural pesticides (Saada et al, 2003; Terlecka, 2005; Baig et al, 2010). The primary source of arsenic contamination is natural dissolution, which results from natural reactions with arsenic bearing minerals (Terlecka, 2005; Baig et al, 2010). For example, deep groundwater arsenic concentration is often controlled by dissolution of arsenic-rich sulfide minerals (Terlecka, 2005). Because arsenic is a known carcinogen, the US EPA (2002) recommends a drinking water limit for arsenic of 10ppb.

Many illnesses and cancer occurrences have recently been linked to arsenic in drinking water wells in Bangladesh and India (Smith, Lingas, and Rahman, 2000; Chowdhury et al, 2000). In a survey of 200 Bangladesh village wells, over 62% had arsenic concentrations over 0.1 ppm (Smith, Lingas, and Rahman, 2000). Another highly affected area of Vietnam was found to have an average arsenic concentration in drinking-water wells of 0.43 ppm (Berg et al, 2001). While arsenic entered into these wells by natural dissolution of minerals, arsenic can also enter groundwater and be collected in soils from different manufacturing and mining processes. For example, a remediation project for a herbicide production plant in Missouri was proposed after a concentration of over 10,000 mg/kg was found in the local soil (Chowdhury, Stanford, and Overby, 2007). The EPA also reported several cases where soil concentration of arsenic was over 200,000

mg/kg (EPA, 2002). Arsenic-contaminated soils can then leach into the groundwater.

Arsenic exists in two common forms in the environment: arsenite As(III) and arsenate As(V). Organic complexes of arsenic can also be found in the environment, but occur in negligible concentrations and are much less toxic than the inorganic forms (Terlecka, 2005). Recent studies indicate that As(III) is more toxic than As(V) (Mandal et al, 2005; United Nations Synthesis Report on Arsenic in DrinkingWater, 2001). However, in most natural and contaminated waters, As(V) is found in higher concentrations than As(III), with As(V) concentrations sometimes up to 90% more than that of As(III) (Smedley and Kinniburgh, 2002; Pettine et al, 1992).

Redox potential and pH are the most important factors controlling arsenic speciation in water (Terlecka, 2005). In oxidizing conditions and at a pH of less than 6.9, the predominant species is $H_2AsO_4^-$. In basic conditions (i.e. pH>7), the dominant species is $HAsO_4^{-2}$. Under very acidic conditions H_3AsO_4 may exist, while at highly alkaline conditions AsO_4^{3-} may be present.

One method which has been tested for arsenate removal is coagulation/flocculation and electrocoagulation (Baskan and Pala, 2010; Ali et al, 2012). For the coagulation process, aluminum sulfate is used as the coagulant which absorbs and then separates As(V) from the water (Baskan and Pala, 2010). Electrocoagulation works in a similar fashion, but uses an iron anode and zinc cathode to attract As(V) (Ali et al, 2012).

Most arsenic removal studies, however, focus on the use of effective sorbents for the removal of arsenic species. The sorbents that have been developed and tested for

As(V) removal and immobilization include metal oxide/hydroxide (Zhang et al, 2010), zero-valent iron (Biterna et al, 2007; Farrell et al, 2001; Melitas et al, 2002), activated carbon (Liu et al, 2010), modified red muds (Zhang et al., 2008; Genc and Tjell, 2003), hydrated ferric oxide polymers (Zhang et al, 2008), as well as synthesized nano materials (Jegadeesan et al, 2005; Hristovski et al, 2008).

2.5 Surfactant-modified zeolites and heavy metal removal

Surfactant-modified zeolites have been shown to be effective means for both chromate and arsenate removal (Li and Bowman, 1998; Yusof and Malek, 2009; Leyva-Ramos et al, 2008; Zeng et al, 2010; Chutia et al, 2009; Li et al, 2007). Other materials such as siderite (Guo et al, 2007) and activated carbon (Leyva-Ramos, 2007) have been tested to remove these contaminants with relatively little removal success compared to modified zeolites. Many researchers have successively used the surfactant HDTMA to modify natural zeolite to remove chromate (Leyva-Ramos et al, 2008; Li, Anghel and Bowman, 1998; Li and Hong, 2009) as well as arsenate (Mendoza-Barron, 2011; Li et al, 2007). Likewise, HDTMA has been used to coat synthetic zeolites for the removal of arsenic and chromium (Shevade and Ford, 2004; Yusof and Malek, 2009). Synthetic zeolites are materials created from the hydrothermal crystallization of aluminosilicate gels (Georgiev et al, 2009). These synthetic materials can have different properties based on the crystallization time, temperature during crystallization, or the composition of the reaction mixture (Georgiev et al, 2009). While HDTMA treated synthetic zeolites have shown significant removal of contaminants (a capacity of 17.92mmol/kg on SMZY-50-S zeolite for arsenate and a capacity of 30.77 mmol/kg on SMZY-200-S for chromate), they are expensive to produce and not as economically suitable for large-scale contamination

removal as treated natural zeolites.

GSMZ is relatively cheap to produce. Natural zeolites typically cost about $30 to $70 per metric ton, depending on the zeolite type and the grain size mined (Virta, 1999). While HDmim is rather new to the market, this group of green solvents is being produced at industrial scales by companies such as iolitec. Hence, GSMZ has the potential to be a cost effective alternative to other materials such as zero-valent iron for field-scale remediation.

3. OBJECTIVE

The main objectives of this study include: 1) the development of an environmentally friendly filtration media (GSMZ) to use for the removal of cationic contaminants (specifically chromate and arsenate); 2) determine how pH and ionic strength effect sorption characteristics for both chromate and arsenate; 3) determine the rate at which adsorption occurs with kinetics experiments; 4) determine the sorption capacity and sorption behavior from batch experiments; 6) utilize the Langmuir competition model to examine sorption behavior and anion competition.

4. MATERIALS AND METHODS

4.1 Natural zeolite characterization

The natural zeolite used in this research was obtained from the St. Cloud Mine which is located in Winston, NM. The zeolite from this mine has been thoroughly characterized in previous surface modification studies: the external cation exchange capacity (ECEC) is 90-110 meq/kg and the external surface area is ~15.7 m^2/g, resulting in an external surface charge density of about -e/26 $Å^2$ (Li, 1998). For the kinetics, isotherm batch experiments, as well as the column experiments, a grain size of 14-40 mesh size was used.

4.2 Preparation of GSMZ

The natural zeolite was modified by the green solvent, HDmim which was obtained from io-li-tec. A solution of approximately 70mM HDmim was made and then mixed with natural zeolite at a liquid to solid ratio of 3:1. In each 50 mL centrifuge tube, 10 grams of natural zeolite and 30 mL of 70 mM HDmim solution were mixed on a rotating mixing table. After 24 hours, the tubes were removed and centrifuged. After the excess surfactant solution was decanted, the zeolite was rinsed and centrifuged twice with nanopure water. The modified zeolite was then dried in an oven set at approximately 60° C.

4.3 Chromate adsorption kinetics

Batch adsorption experiments were performed with GSMZ and a chromate solution (150 mg/L) at a range of pH and ionic strength conditions. The chromate solution was made using sodium chromate terahydrate from Alfa Aesar. The pH of the

background solutions varied between 4 and 9. The pH 4 buffer was 1 mM CH_3COONa, the pH 7 buffer was 0.1 mM NaHCO3, and the pH 9 buffer was 1 mM $NaHCO_3$. The ionic strengths were 5, 20, and 100 mM (adjusted using NaCl), respectively. To determine the kinetics, mixtures of a known amount of GSMZ (1g) and a fixed volume of chromate solution (10 mL) with a particular concentration (150 mg/L) were mixed on a rotating mixing table for varying amounts of time (0, 1/60, 1/30, 1/12, 1/4, 1/2, 1, 2, 4, 6, 22, 24 hours). The mixture was then filtered through 0.2 micrometer cellulose acetate membrane filters (VWR International).

The supernatant of the chromate solution was analyzed using a modification of the EPA method 7196A, in which a diphenyl carbazide solution is mixed with the supernatant and 0.2 M hydrochloric acid, revealing a pink color (Li and Zou 1999). The absorbance was then quantified using a UV-Vis Spectrophotometer (UV-1601 UV-Visable Spectrophometer by Shimadzu) at a wavelength of 540 nm. The amount of adsorbed chromium was determined based on the mass balance of chromium added to each tube.

4.4 Chromate adsorption isotherms.

Similar to the kinetics study, a known amount of GSMZ (1 g) was mixed with 10 mL of chromate solution at varying concentrations. For chromate, the solution concentrations ranged between 0 and 250 mg/L. The mixtures of chromate solution and modified zeolite were then thoroughly mixed on an end-to-end mixing table for 24 hours. The mixture was then filtered and the supernatant was analyzed for contaminant concentration using the EPA method described above. The amount of chromate absorbed was determined by the difference between the initial and final concentrations. Duplicate

experiments were performed for each pH and ionic strength combination. There were a total of 9 different experiments: 3 different ionic strengths (5, 20, 100 mM) were tested for each pH value (4, 7, 9).

4.5 Arsenate adsorption kinetics

Batch adsorption experiments were also performed with arsenate and GSMZ at different pH and ionic strength combinations. Like the chromate experiments, the pH ranged between 4 and 9 (using the same buffers as described above). The ionic strength for the arsenate experiments differs in that it ranges from 1 to 20 mM (1, 5, and 20 mM, adjusted using NaCl). The arsenate solution was made using sodium arsenate heptahydrate. Kinetics experiments for arsenate were performed in the same way as for chromate. Mixtures of a known amount of GSMZ (1g) and a fixed volume of arsenate solution (10 mL) with a particular concentration (150 mg/L) were mixed on a rotating mixing table for varying amounts of time (0, 1/60, 1/30, 1/12, 1/4, 1/2, 1, 2, 4, 6, 22, 24 hours). The mixture was then filtered through 0.2 micrometer cellulose filters and diluted with 5% nitric acid, as acidic conditions are necessary for analysis by Atomic Adsorption Spectrophotometry (AAS). The supernatant for arsenate solutions were analyzed using the AAS Spectrophotometer (Thermo Scientific). All experiments were done in duplicate.

4.6 Arsenic adsorption isotherms.

The arsenate isotherm experiments were performed in the same way as the chromate experiments, with the exception of different ionic strength values as described above. One gram of GSMZ was mixed with 10 mL of arsenate solution at varying

concentrations. For arsenate, solution concentrations ranged between 0 and 750 mg/L. The mixture was then thoroughly mixed on a rotating mixing table for 24 hours. After filtering the samples, the supernatant was analyzed using AAS. Duplicate experiments were performed for each pH and ionic strength combination.

4.7 Zeta potential tests

In order to determine whether surface charge of the GSMZ changed with respect to pH, zeta potential tests were conducted using a Brookhaven Instruments Corporation "Zeta Plus" analyzer. Half of a gram of GSMZ was suspended in 20 mL of solutions with pH of 4, 5.5, 7, 8, and 9 and was allowed to settle for about 30 minutes. Each sample was then tested three times, with the machine taking 5 readings for each run. The output data came in the form of mobility, zeta potential, and conductance.

5. RESULTS AND DISCUSSION

5.1 Chromate kinetics

The influence of contact time on the sorption of chromate is shown in Figures 1 and 2. Chromate attaches to the cationic sites either in the form of $HCrO_4^-$ or CrO_4^{2-}, depending on the pH. The main mechanism for chromate removal can be attributed to anion exchange at the HDmim tail sites (Li. et al, 1998).

The kinetics study indicates that sorption occurs quickly. The majority of sorption (about 50%) happens in less than one minute. After one minute, sorption continues to increase, but does so more gradually. For all conditions, the peak of adsorption is reached after approximately 2 hours. After this time, capacity is reached, with sorption hitting a maximum. However, an increase in contact time after just 15 minutes has little effect on the sorption capacity. Initial sorption rates for chromate are very high, as there are many available sites for attachment. As the sites begin to fill, the adsorption rate slows.

The fast sorption rate for HDmim zeolite is advantageous for its use as a contaminant filter for drinking water. Because the majority of chromium was captured in 2 minutes or less, the contact time between zeolite and contaminated water could be minimal in a filtration system.

The kinetics experiments also indicate two emerging trends which are replicated in the batch adsorption isotherm experiments. The pH of solution tested has little effect on the sorption maximum. This is shown in Figure 2, which displays the results of kinetics for a single ionic strength (20mM) with different pH (4, 7, 9). The results show a

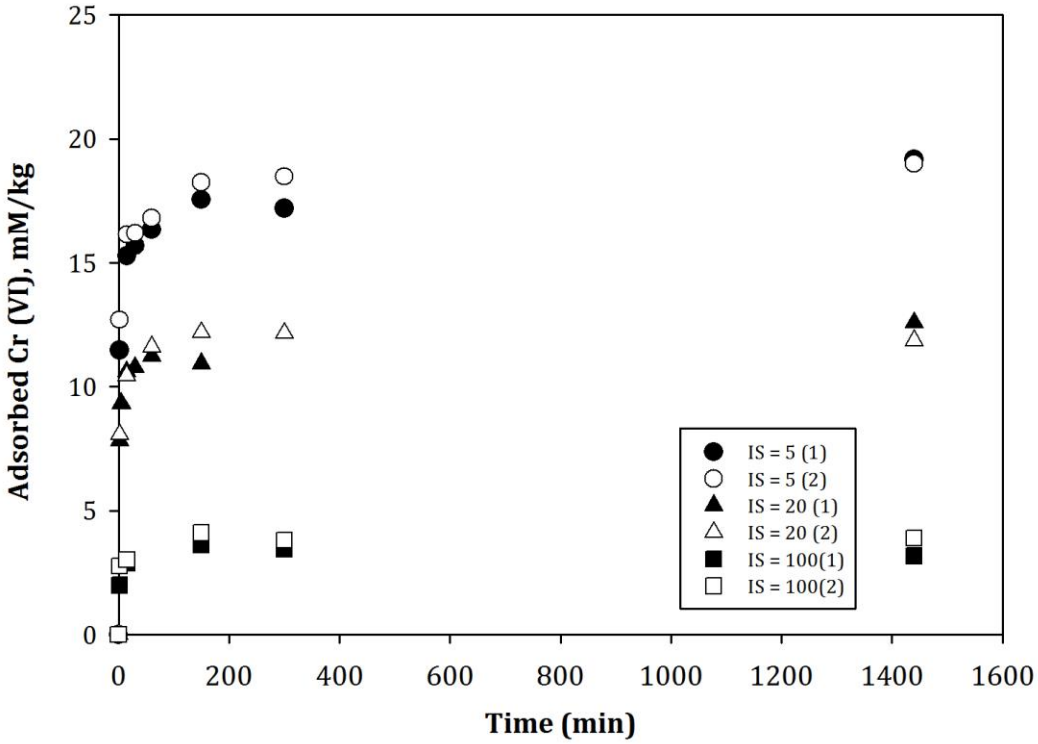

Figure 1. Cr(VI) kinetics for different ionic strength at pH 7.

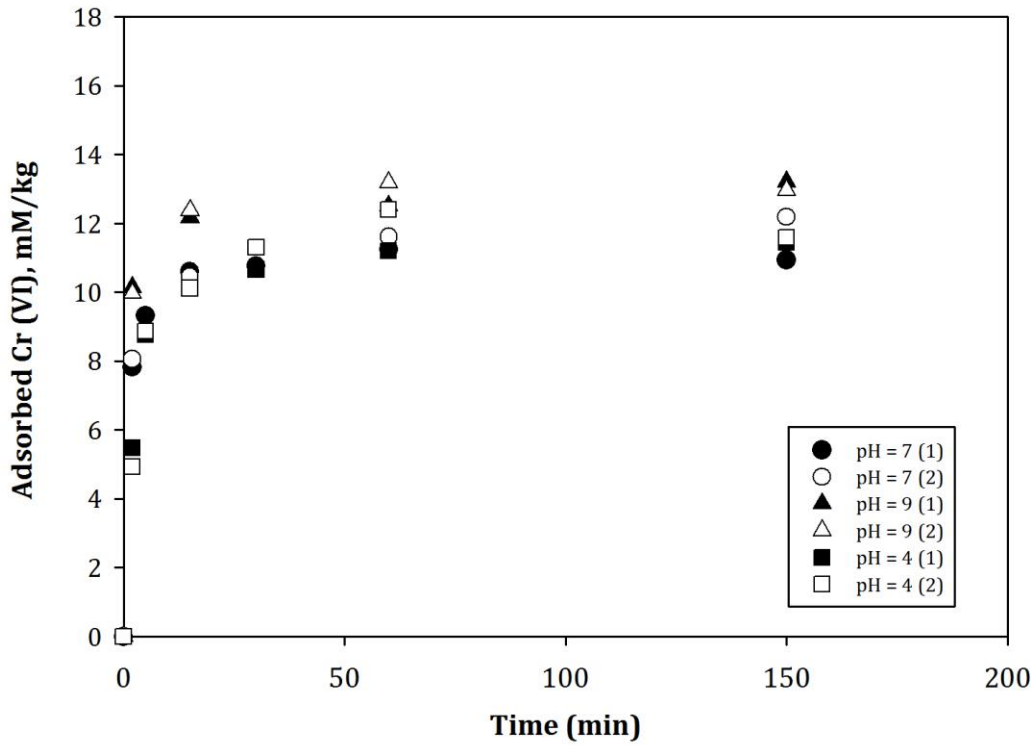

Figure 2. Cr(VI) kinetics for ionic strength 20mM, at different pH.

very similar behavior. The second trend is that ionic strength is an important factor for the maximum removal of chromate. Figure 1 displays the sorption as a function of time with different ionic strengths. The square symbols, which represent an ionic strength of 100 mM show an adsorption maximum about 75% less than the 5 mM kinetics experiments which are represented by the circle symbols.

5.2 Chromate Isotherms

The Langmuir competition model was used to account for the amount of competition between different anions in solution, namely chromate and chloride. The Langmuir competition model is described by the following equation:

Equation 1. $$S = \frac{K_{Cr} S_m C_{Cr}}{1 + K_{Cr} C_{Cr} + K_{Cl} C_{Cl}}$$

where S is the amount of Cr sorbed on the solid surfaces at equilibrium (mmol/kg), S_m is sorption capacity (mmol/kg), C_{Cr} is the equilibrium liquid concentration of Cr(VI) (mmol/L), C_{Cl} is the equilibrium liquid concentration of Cl^- (mmol/L), K_{Cr} is the Langmuir coefficient for chromate (L/mmol), and K_{Cl} is the Langmuir coefficient for chloride (L/mmol).

A code was created to solve for S_m, K_{Cr}, and K_{Cl} for each set of experiments run for the three pH values. The model uses the observed data for the three ionic strengths (5, 20, and 100 mol) and converges to the sorption maximum. Table 1 shows the values obtained for S_m, K_{Cr}, and $K_{Cl.}$

From this data, model curves were fit to the experimental output (Figures 3, 4, and 5). The Langmuir curves represent an equilibrium between the amount of contaminant in the aqueous phase versus the amount of sorbed contaminant at some equilibrium point.

Langmuir Competition Model results for chromate			
pH 4	Sample set 1	Sample set 2	Average
Sm	27.27	25.73	26.50
K_{Cr}	196.33	222.22	209.28
K_{Cl}	39.61	38.06	38.83
pH 7	Sample set 1	Sample set 2	Average
Sm	26.52	25.86	26.19
K_{Cr}	133.27	190.75	162.01
K_{Cl}	26.23	34.95	30.59
pH 9	Sample set 1	Sample set 2	Average
Sm	29.49	29.62	29.55
K_{Cr}	177.90	42.13	110.02
K_{Cl}	27.24	6.68	16.96

Table 1. Results for Langmuir competition model with chromate and chloride. Where Sm is the sorption capacity (mM/kg), K_{Cr} is the Langmuir coefficient for chromate (L/mM), and K_{Cl} in the Langmuir coefficient for chloride (L/mM).

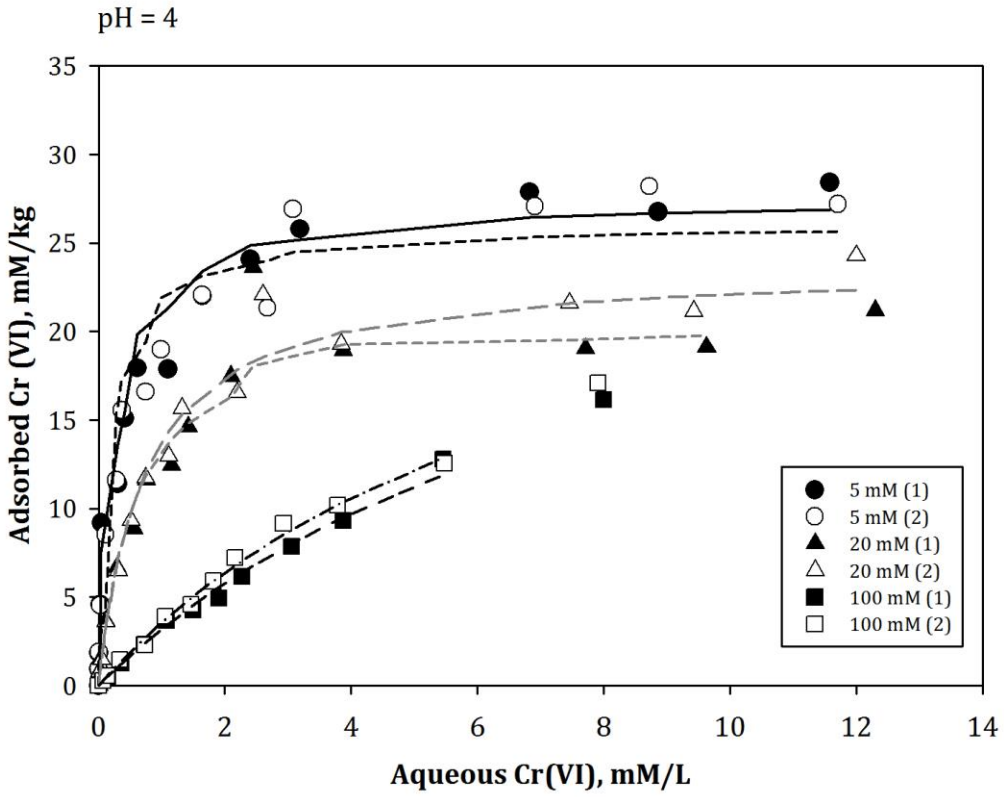

Figure 3. Cr(VI) batch experiment data for pH 4 at different ionic strength, with fitted model Langmuir curves.

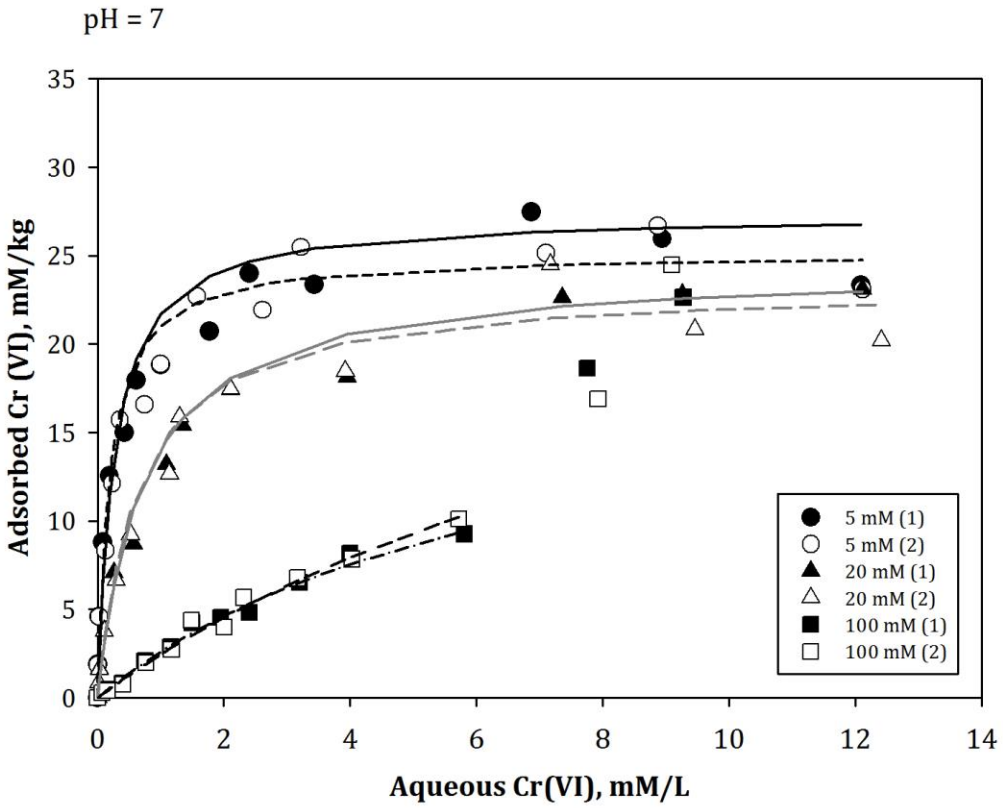

Figure 4. Cr(VI) batch experiment data for pH 7 at different ionic strength, with fitted model Langmuir curves.

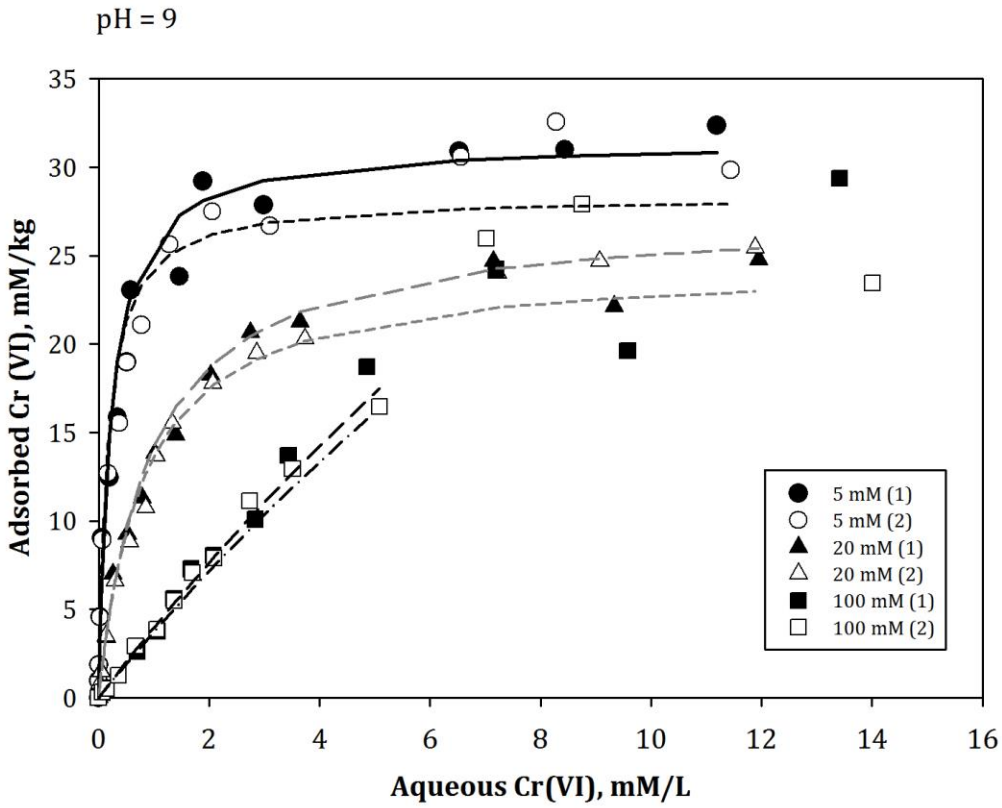

Figure 5. Cr(VI) batch experiment data for pH 9 at different ionic strength, with fitted model Langmuir curves.

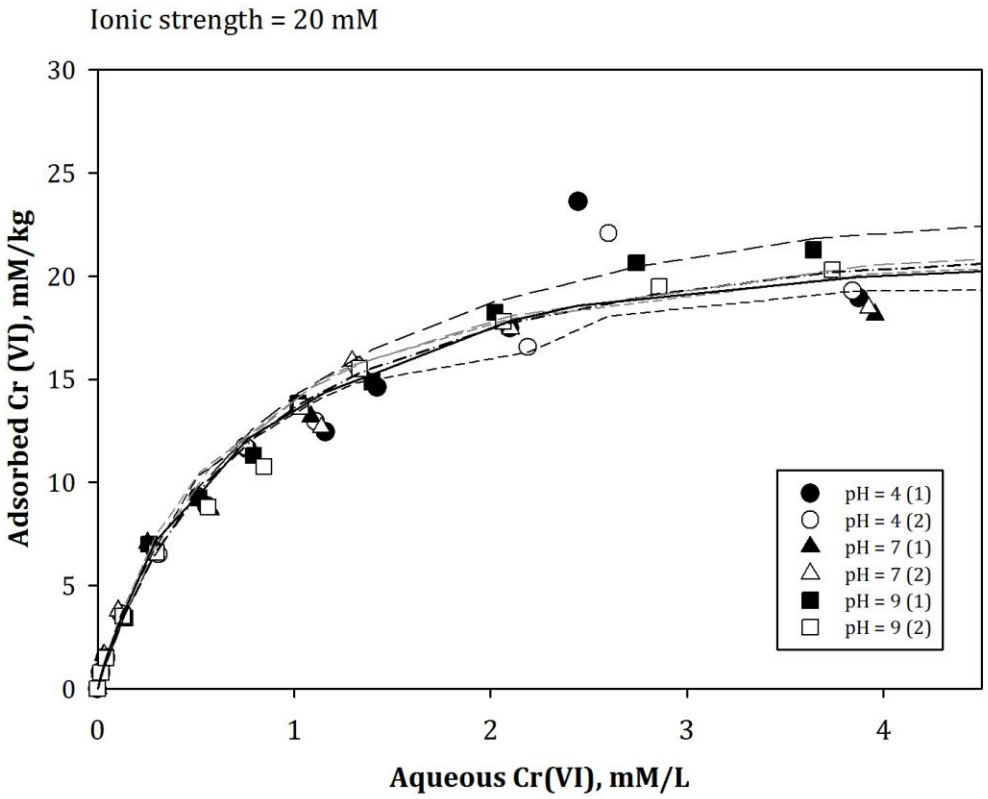

Figure 6. Cr(VI) batch experiment results for different pH at ionic strength 20mM, with fitted model Langmuir curves.

Initially, the adsorption sites fill up quickly and as sites become less available, the sorption slows. The plateaus we observe in our isotherm experiment graphs depict the sorption maximum at which the zeolite can not adsorb any more chromate.

5.3 Effect of pH on the adsorption capacity of chromate

Our results show that pH has very little effect on the adsorption capacity for HDmim zeolite (Figure 6). This behavior indicates that the sorption of Cr(VI) is not dependent on the predominant species present at each pH.

Previous work using HDTMA modified zeolite suggested that chromate sorption was dependent on pH because different chromate ions exist in solution depending on the pH. Yusof and Malek (2009) found that the highest sorption capacity occurred at a pH of 3 and sorption capacity showed a general trend of decreasing as pH increased.

The equilibrium for chromate speciation is described by the following:

$HCrO_4^- \leftrightarrow CrO_4^{2-} + H^+$, pKa = 5.9

$H_2CrO_4 \leftrightarrow HCrO_4^- + H^+$, pKa = 4.1

$Cr_2O_7^{2-} + H_2O \leftrightarrow 2HCrO_4^-$, pKa = 2.2

At lower pH (below 7), the dominant species is a univalent form ($HCrO_4^-$). Because this species only has one negatively charged location, it is believed that it only requires one exchange site on the surface of the zeolite (Yusof and Malek, 2009). Meanwhile, at higher pH, the dominant species is a divalent form (CrO_4^{2-}) which requires two of the positively charged sites on the zeolite. This argument suggests that chromate sorption should be highest at lower pH values. This, however, was not the case observed in our work.

The maximum sorption values we obtained were for the lowest ionic strength used

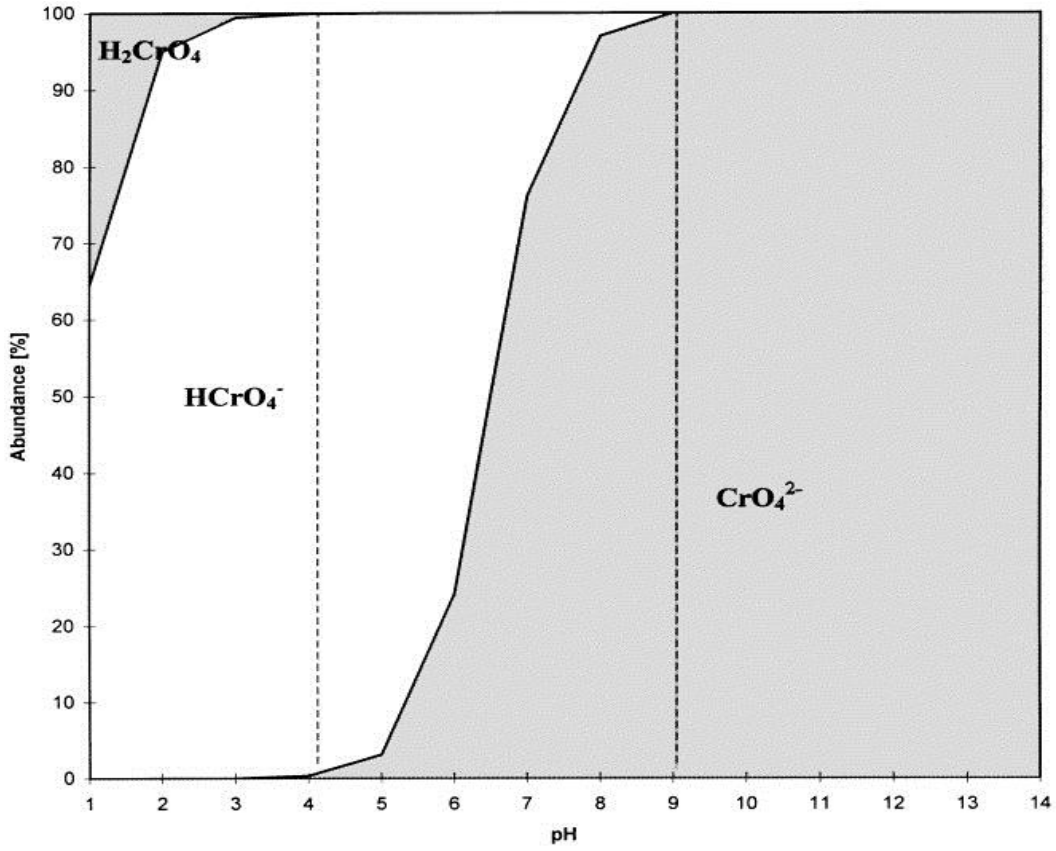

Figure 7. The speciation of chromate at different pH. Dotted lines represent the pH range tested in this study.

(5mM). In general, the S_m value is approximately 26 mM/kg (Table 1). A slightly higher value of about 29 mM/kg was achieved at pH 9, but in general the trend does not change significantly depending on the pH. This is exemplified by Figure 6 which shows the three pH experiments for the single ionic strength of 20 mM. The modeled Langmuir curves nearly lie atop one another.

Zeta potential tests were conducted within the pH range used in this study to determine whether the surface charge of the GSMZ was affected by different pH. Results from the zeta potential test are displayed in Table 2. The results show that there was little difference in the charge of the zeolite surface within the pH range tested in this study. All charges were positive, with values ranging from 30.9 to 40.7. The zeta potential value did decrease slightly as the pH increased to 9. However, the similar charges on the zeolite for each pH suggests that if the chromate speciation is not important for the sorption, the sorption maximum should not be affected by the pH of the solution tested.

5.4 Effect of ionic strength on adsorption capacity for chromate

Unlike pH, the ionic strength of the solution plays an important role in the observed sorption capacity. Figures 3, 4, and 5 show that ionic strength has a strong influence on the Cr(VI) removal using GSMZ. As the ionic strength increases from 5 mM to 100 mM, the sorption capacity notably decreases. NaCl was used to adjust the ionic strength after the buffers were added to stabilize the pH. At the higher ionic strength, more chloride anions are in solution, which compete with the chromate anions for the positively charged tail sites at the surface of the zeolite.

Although other researchers have noted this same effect on ionic strength and coexisting anions, the Langmuir competition model has not been applied to experimental

Zeta potential tests with HDmim modified zeolite and different pH solutions			
pH 4	Mobility	Zeta Potential	Conductance
Run 1	2.9	38.56	167
Run 2	3.13	41.67	161
Run 3	2.52	33.5	133
Total Average	2.85	37.91	153.67
PH 5.5	Mobility	Zeta Potential	Conductance
Run 1	2.18	29.02	141
Run 2	3.15	41.82	136
Run 3	3.85	51.18	136
Total Average	3.06	40.67	137.67
PH 7	Mobility	Zeta Potential	Conductance
Run 1	3.26	43.31	156
Run 2	3.01	40.09	171
Run 3	2.68	35.69	168
Total Average	2.98	39.70	165
PH 8	Mobility	Zeta Potential	Conductance
Run 1	2.69	35.79	155
Run 2	2.72	36.22	150
Run 3	2.29	30.35	157
Total Average	2.57	34.12	154
PH 9	Mobility	Zeta Potential	Conductance
Run 1	2.21	29.29	339
Run 2	2.44	34.43	341
Run 3	2.33	30.97	340
Total Average	2.33	31.56	340

Table 2. Zeta potential results for GSMZ at different pH ranging from 4 to 9.

data previously (Zeng et al, 2010; Li, Anghel, and Bowman, 1998). Zeng and others (2010) found that sulfate and phosphate ions had the greatest effect on the reduction of Cr(VI) removal on HDTMA modified clinoptilolite, while chloride, nitrate, and calcium ions had little impact on their experimental removal. Li, Anghel, and Bowman (1998) noted a similar occurrence with their HDTMA zeolite experiments. They found that an increase in sulfate concentration resulted in less chromate sorption capacity, and that compared to 0.1mM sulfate, the 10mM sulfate results showed a reduction of nearly half of the chromate sorption capacity (Li, Anghel, and Bowman, 1998).

The Langmuir coefficient reflects the affinity of the solute for the sorption sites. The larger the K value, the higher affinity an anion has for the sorption sites on the zeolite. The results for Langmuir coefficients for both chromate and chloride are displayed in Table 1. Although the actual estimated values vary for each pH, for each case, K_{Cr} is more than 5 times greater than K_{Cl}. This suggests that although the chloride anions are indeed competing for the surface sites, and do reduce the overall sorption maximum, the chromate anions still have a higher affinity for the sites. Because the presence of competing anions affects the chromate sorption significantly, we can deduce that the sorption mechanisms for both species are similar.

5.5 GSMZ compared to SMZ results, chromate

To determine whether the environmentally friendly Green Solvent Modified Zeolite (GSMZ) is a viable option for field use, we can compare our results to those obtained in previous work. Many previous researchers have performed similar experiments with modified zeolites. Many such experiments utilize Surfactant Modified

Zeolite (SMZ) which is modified with the surfactant HDTMA. Several research groups have found success when using these materials.

In our work, the highest sorption maximum for GSMZ was achieved at the lowest ionic strength for the chromate experiments. Data suggests an Sm value generally ranging between 26 and 29 mM/kg. Using the same loading level of 200 mM/kg of surfactant, Li and Bowman (1998) achieved a sorption capacity of 10 mM/kg. For this case, the GSMZ removes nearly 3 times as much contaminant compared to SMZ. Using SMZ, Bowman (2005) found a sorption capacity of 14mM/kg for chromate in distilled water. Research by Yusof and Malek (2009) used HDTMA modified synthetic zeolites in a similar experimental design. This work determined a very similar sorption capacity to that which we observed, varying between 27.1-30.77 mM/kg. The drawback of the material used by Yusof and Malek however, is that synthetic zeolites are more difficult and expensive to produce (Yusof and Malek, 2009; Georgiev, 2009).

Other research groups have found even higher sorption capacity using a natural zeolite coated with HDTMA (Leyva-Ramos et al, 2008; Zeng et al, 2010). Leyva-Ramos and others (2008) determined a sorption maximum of 79 mM/kg at pH 6. Likewise, using a HDTMA modified clinoptilolite, Zeng and others (2010) found a sorption maximum of 68.3 mM/kg at pH 3. These numbers are twice as large as those observed in this study. Such large values are rather unrealistic, however. Both studies reported a HDTMA loading level of about 180 mM/kg on the modified zeolite. Because two carbon chains are needed to create one positive tail site, the absolute maximum sorption capacity would be 90 mM/kg. The two studies achieved 76% coverage of Cr(VI) on zeolite at equilibrium (Zeng et al, 2010) and 88% coverage of Cr(VI) at maximum (Leyva-Ramos

et al, 2008). Such high attachment is not realistic for this modified media.

5.6 Arsenate kinetics

Both batch kinetics and isotherm experiments with arsenate showed similar trends as those performed with chromate. While ionic strength did have an effect on the maximum sorption because of anion competition, pH played a small role in the removal of arsenic.

The influence of contact time on the sorption of arsenate is shown in Figures 8 and 9. Arsenate attaches to the cationic sites either in the form of $H_2AsO_4^-$ or $HAsO_4^{-2}$, depending on the pH. Like chromate, the main mechanism for arsenate removal can be attributed to anion exchange at the HDmim tail sites (Li et al., 2007).

The kinetics study indicates that arsenate sorption is occurring very rapidly, even faster than chromate sorption. The majority of sorption (about 85%) happens in less than one minute (Figure 8). After one minute, sorption continues to increase, but it does so more gradually. For all conditions, the peak of adsorption is reached very quickly after approximately 5 minutes. After this time, capacity is reached, with sorption hitting a maximum.

Similar to the findings related to chromate adsorption, the kinetics experiments also indicate two emerging trends which are replicated in the batch adsorption isotherm experiments. The pH of the solutions tested had little effect on the sorption maximum. This is shown in Figure 9, which displays the results of kinetics for a single ionic strength (20 mM) with different pH (4, 7, 9). The results are very similar. The second trend is that ionic strength is an important factor for the maximum removal of arsenate. Figure 8 displays the sorption as a function of time at pH 7, with three different ionic

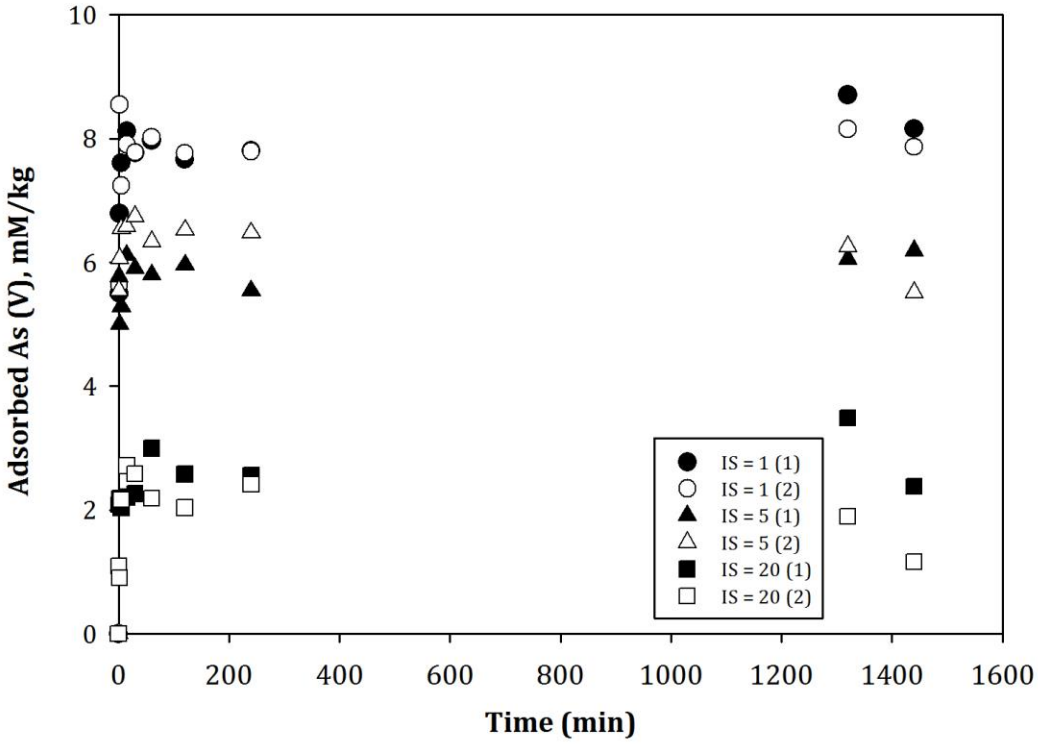

Figure 8. Kinetics data for arsenate at pH 7 with different ionic strength.

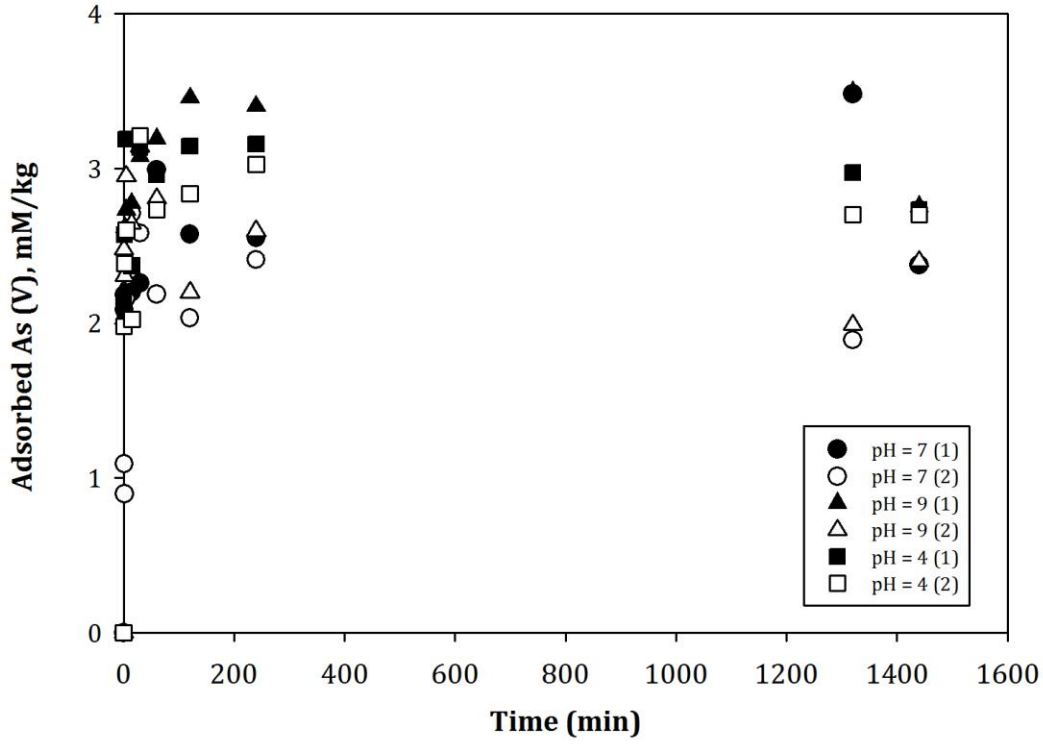

Figure 9. Kinetics data for arsenate at ionic strength 20mM at different pH.

strengths. The square symbols, which represent anionic strength of 20 mM show an adsorption maximum about 70% less than the 1mM kinetics experiments, which are represented by the circle symbols.

5.7 Arsenate Isotherms

The Langmuir competition model was applied to experimental data for arsenate to account for the amount of competition between different anions in solution.

The same code used for the chromate data was used, following the Langmuir Competitive model, to solve for S_m, K_{As}, and K_{Cl} for each set of experiments run for the three pH values. Values obtained from the model are shown in Table 3. The model also provided a good fit for the experimental arsenate data, as shown in Figures 10, 11, and 12.

5.8 Effect of pH on the adsorption capacity of arsenate

Results for batch experiments used to determine the efficiency of GSMZ for arsenate removal over a pH range from 4-9 are shown in Figures 10, 11, and 12 . It is clear that pH does not play a large role for sorption of arsenate. For the pH range tested, the average sorption capacity was about 12 mmol/kg. A slightly lower sorption capacity was observed at pH 7 however, with a capacity of about 10 mmol/kg.

The speciation of As(V) at different pH is described by the following:

$H_3AsO_4 \leftrightarrow H_2AsO_4^- + H^+$ pKa = 2.3

$H_2AsO_4^- \leftrightarrow HAsO_4^{2-} + H^+$ pKa = 6.8

$HAsO_4^{2-} \leftrightarrow AsO_4^{3-} + H^+$ pKa = 11.6

At basic pH (above pH 7), the predominant species is the divalent form ($HAsO_4^{-2}$). Below pH 7, $H_2AsO_4^-$ is the most prevalent species. Because pH has little effect on the adsorption of arsenate, we can deduce that $HAsO_4^{-2}$ and $H_2AsO_4^-$ have the

Langmuir Competition Model results for arsenate			
pH 4	Sample set 1	Sample set 2	Average
Sm	12.52	12.33	12.42
K_{As}	8.06	5.34	6.70
K_{Cl}	1.69	1.02	1.35
pH 7	Sample set 1	Sample set 2	Average
Sm	9.75	9.99	9.87
K_{As}	17.05	12.56	14.80
K_{Cl}	2.10	1.75	1.93
pH 9	Sample set 1	Sample set 2	Average
Sm	11.26	12.98	12.12
K_{As}	10.67	5.28	7.97
K_{Cl}	1.97	1.30	1.64

Table 3. Results for Langmuir competition model with arsenate and chloride. Where Sm is the sorption capacity (mM/kg), K_{As} is the Langmuir coefficient for chromate (L/mM), and K_{Cl} in the Langmuir coefficient for chloride (L/mM).

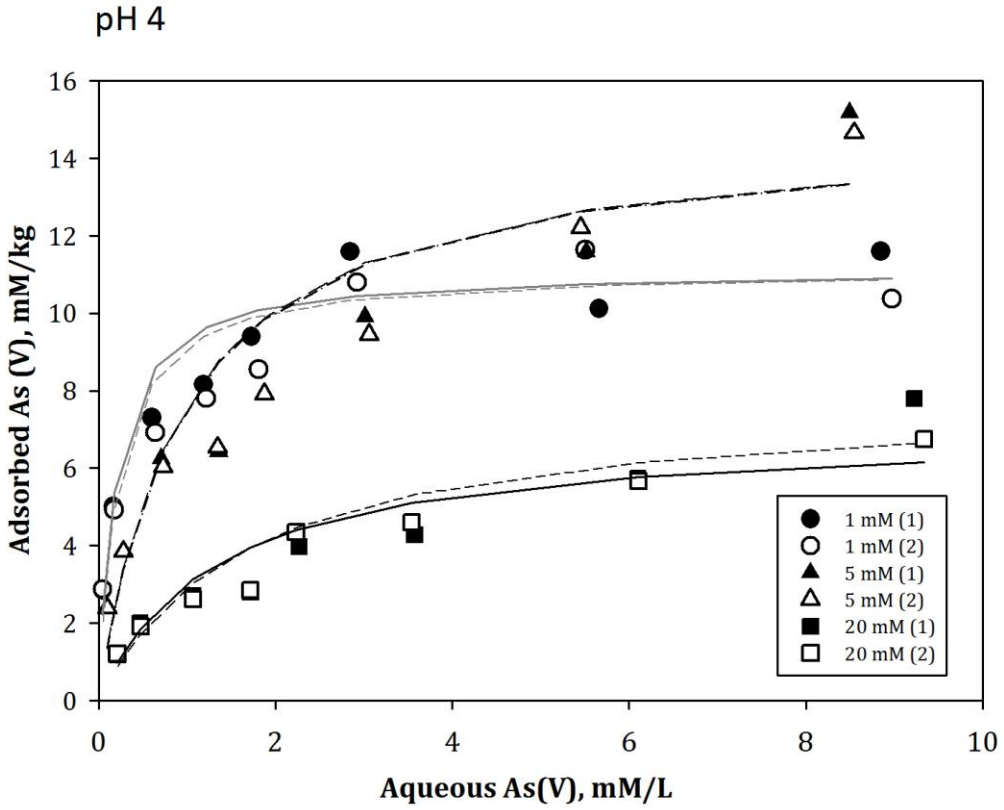

Figure 10. Batch experiment data for arsenate at pH 4 with different ionic strength. Modeled Langmuir curves are fit to data.

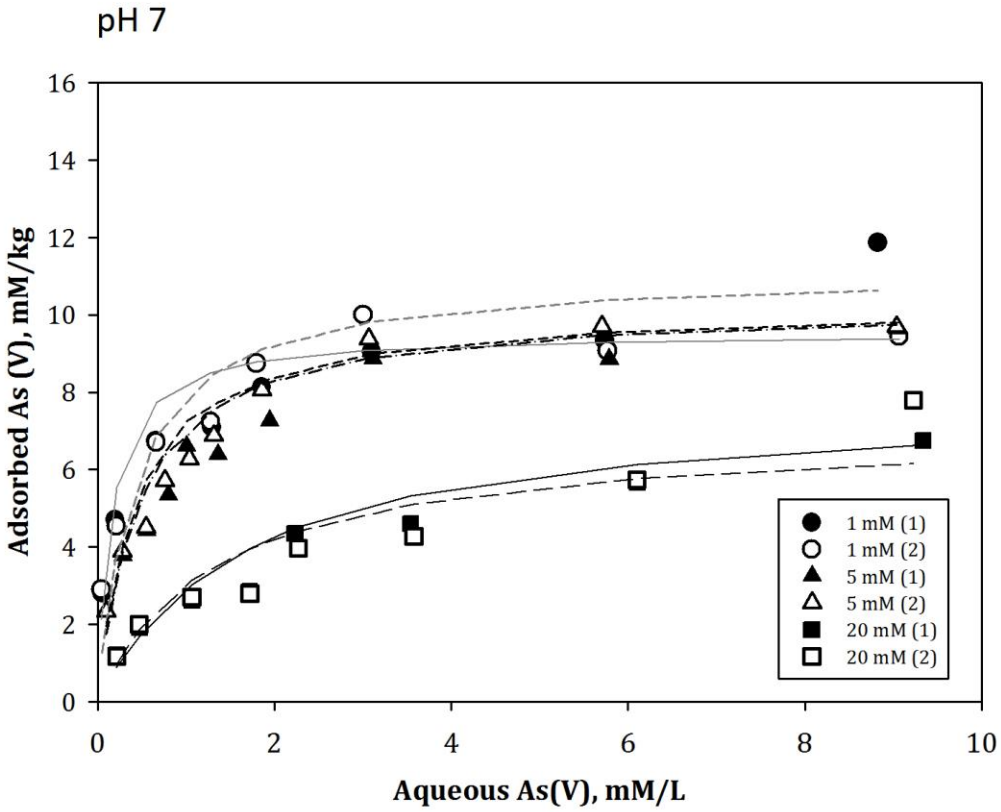

Figure 11. Batch experiment data for arsenate at pH 7 with different ionic strength. Modeled Langmuir curves are fit to data.

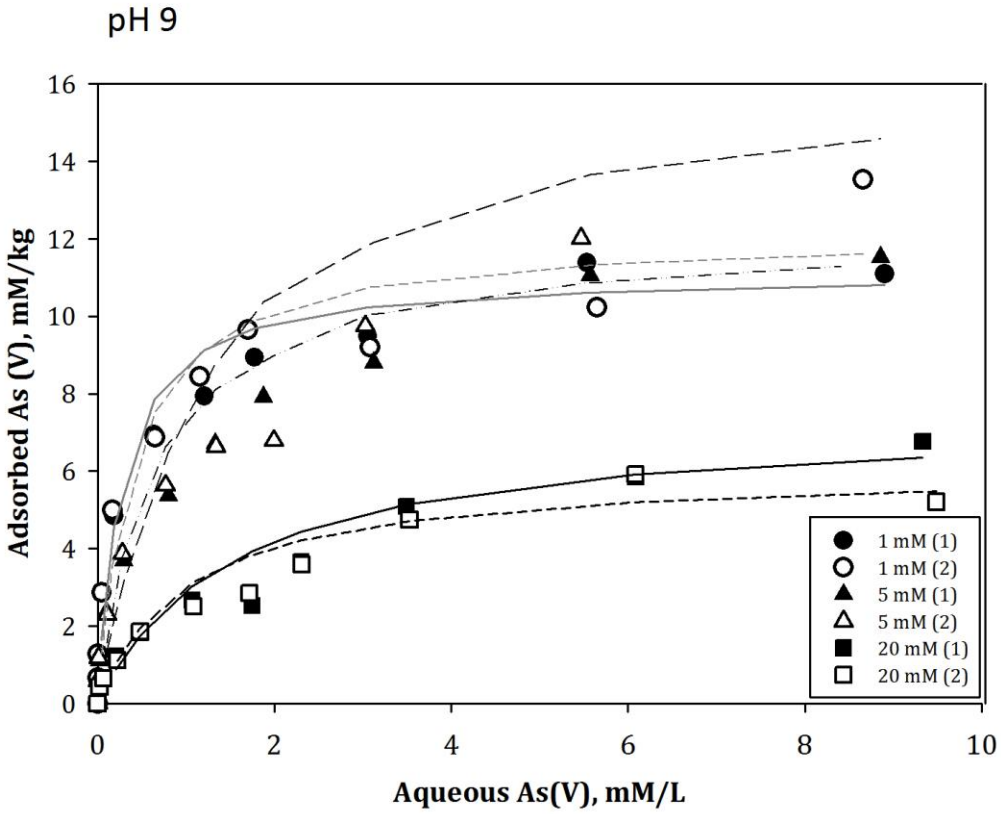

Figure 12. Batch experiment data for arsenate at pH 9 with different ionic strength. Modeled Langmuir curves are fit to data.

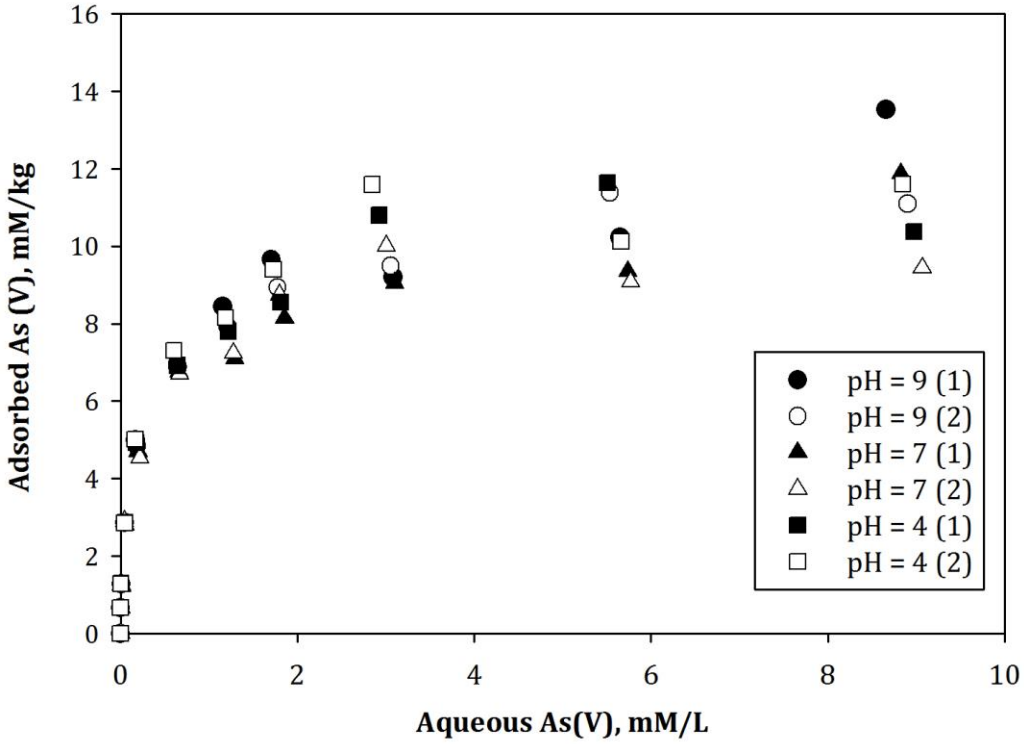

Figure 13. Batch experiment data for arsenate at ionic strength 1mM and different pH.

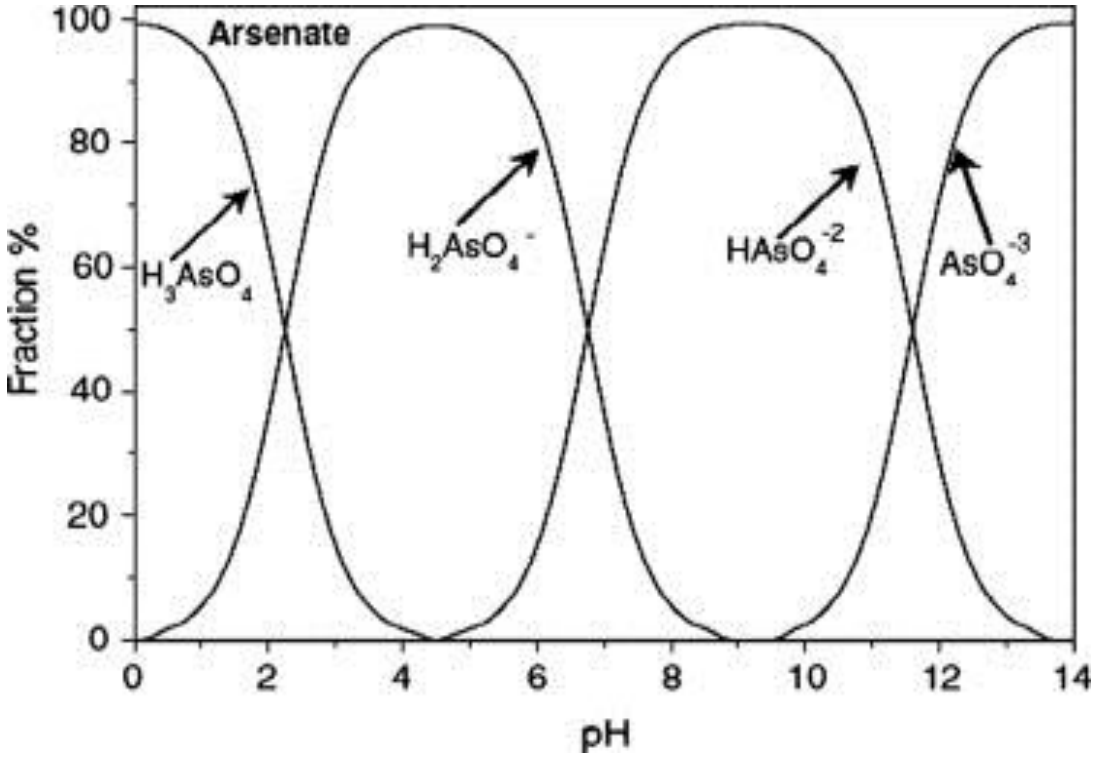

Figure 14. The speciation of arsenate at different pH.

same affinity for the positive tail sites on GSMZ. Both the divalent and univalent form of arsenate are sorbed by anion exchange with the chloride counterions which stabilize the HDmim bilayer.

Other researchers have also observed that pH plays a negligible role for arsenate adsorption to HDTMA modified zeolites and clays (Li et al, 2007; Shevade and Ford, 2004; Chutia et al, 2009). Similar to our results, previous work has found that there is a wide optimum pH range for arsenate removal and that removal is not greatly affected between pH 3-11 (Shevade and Ford, 2004; Chutia et al, 2009).

The previously mentioned zeta potential tests show that within the pH range used in this study, the surface charge of the GSMZ was not affected by different pH (Table 2) The similar charges on the zeolite for each pH suggests that if the arsenate speciation is not important for the sorption, the sorption maximum should then not be affected by the pH of the solution tested.

5.9 Effect of ionic strength on adsorption capacity for arsenate

Similar to the chromate adsorption on GSMZ, arsenate sorption was affected by the ionic strength of the solutions tested. Figures 10, 11 and 12 show that ionic strength has a strong influence on the As(V) removal using GSMZ. As the ionic strength increases from 1 mM to 20 mM, the sorption capacity decreases. Because NaCl was used to adjust the ionic strength after the buffers were added to stabilize the pH, the additional chloride anions in solution increase the competition with arsenate anions for the positively charged tail sites at the surface of the zeolite.

At a concentration of arsenate in solution at 3mM/L or lower, the 1mM ionic strength solution consistently shows a higher sorption maximum compared to the 5mM

ionic strength solution. Above an initial As(V) concentration of 3mM/L however, there often is little difference between the sorption maximum from 1mM or 5mM ionic strength. However, for some cases, the sorption maximum is higher for 5mM. For example, at the pH 4, ionic strength 5mM condition, the sorption maximum is about 2 mM/kg larger than the 1 mM condition. On the other hand, the 20mM ionic strength solutions always show a lower adsorption capacity, with a value of S_m about 40% lower than for 1 or 5 mM.

The results for Langmuir coefficients for both arsenate and chloride are displayed in Table 3. Although the actual estimated values vary for each pH, for each case, K_{As} is more than 4.5 times greater than K_{Cl}. Even though additional chloride anions compete for the positively charged sites, there is still a higher affinity, and thus a preference for sorption of arsenate.

5.10 GSMZ compared to SMZ results, arsenate

To determine whether the environmentally friendly Green Solvent Modified Zeolite (GSMZ) is a viable option for field use for arsenate remediation, we can compare our results to those obtained with previously modified zeolites. Similar work with arsenate removal using HDTMA modified zeolites has been tested in the past (Chutia et al, 2009; Yusof and Malek, 2009; Li et al, 2007; Mendoza-Barron et al, 2010). Our research determined a maximum capacity of about 10-12 mM/kg for arsenate sorbed on GSMZ. Using the same loading level used in this study (200% ECEC), Li and others (2007) observed a sorption capacity of 7.2 mM/kg for arsenate absorped on HDTMA modified zeolite. Yusof and Malek (2009) also found similar sorption capacities to those observed in this study, with sorption maximums on HDTMA modified Na-Y synthesized

zeolite ranging between 9.16-17.04 mM/kg at 200% ECEC.

Other researchers have reported a higher removal of arsenate with HDTMA modified zeolites (Chutia et al, 2009). Chutia and others modified a natural zeolite to 200% ECEC and used arsenate concentrations similar to those used in this study. Chutia and others (2009) reported a sorption capacity of 45.33 mM/kg, which is about 30% greater than that observed in this study. At a loading level of 200% ECEC, this ouput suggests that nearly half of the sorption sites are occupied by arsenate, which is likely an overestimation. Mendoza-Barron and others (2010) reported a much lower capacity of 0.33 mM/kg. However, their work utilized much lower arsenate concentrations (Mendoza-Barron et al, 2009). The concentrations used in this study are large, varying from 5ppm to 750ppm.

6. CONCLUSIONS

Results from this research indicate that of the two parameters tested, ionic strength is much more important for the sorption limitations of the heavy metals arsenate and chromate onto GSMZ. Ionic strength affects the sorption capacity because the additional chloride ions compete for sorption sites on GSMZ. Langmuir competition modeling indicated that even though increasing ionic strength lowers the sorption capacity, the heavy metal ions still have a stronger affinity for the GSMZ sites. Meanwhile, pH appeared to have little effect on the sorption capacity. Zeta potential tests indicated that the surface of GSMZ is consistently positive for the pH range tested, so that regardless of speciation, the negatively charged arsenate and chromate will attach in a similar way.

Furthermore, our results show that GSMZ could be a useful material to utilize in groundwater remediation. When reviewing other results for modified zeolites in heavy metal removal, it is clear that GSMZ performs as well, if not better than the previously utilized SMZ. GSMZ would be well suited for use in a permeable reactive barrier at sites contaminated with heavy metals. Additionally, this material has possible applications for drinking water filtration media due to its rapid sorption kinetics.

7. FUTURE WORK

Future work with HDmim modified zeolite (GSMZ) may focus on desorption characterization. Desorption of the surfactant itself would be useful information. Studies with HDTMA indicate that there is very little desorption of the surfactant once the bilayer has been created (Li et al, 1998). However, such investigations with HDmim have not been conducted. Perhaps more important may be the study of desorption of contaminants from GSMZ. In order to be an effective adsorption and filtration media, the GSMZ must retain whatever contaminants are initially sorbed. Such studies would help determine the usefulness and longevity of GSMZ as a filtration media. Furthermore, research should be conducted using GSMZ with other ions in solution. Many impurities exist in natural water which could have an even greater effect on the sorption capacity of Cr(VI) and As(V) than ions such as sodium and chloride.

References

Agency for Toxic Substances and Disease Registry. 2011. Substance Priority List.

Ali, I., Khan, T., and Asim, M. 2012. Removal of arsenate from groundwater by electrocoagulation method. Environmental Science and Pollution Research International **19.5**: 1668-1676.

Apreutesei, R., Catrinescu, C., Theodosui, C., 2008. Surfactant-Modified Zeolites for Environmental Applications in Water Purification, Environmental Engineering and Management Journal **7**: 149-161.

Baig, J., et al., 2010. Speciation and evaluation of Arsenic in surface water and groundwater samples: A multivariate case study. Ecotoxicology and Environmental Safety **73**: 914-923.

Baskan M. and Pala A. 2010. A statistical experiment design approach for arsenic removal by coagulation process using aluminum sulfate. Desalination **254**: 42–48.

Bautistatoledo, I., J. Riverautrilla, M. A. Ferrogarcia, and C. Morenocastilla. 1994. Influence of the Oxygen-Surface Complexes of Activated Carbons on the Adsorption of Chromium Ions from Aqueous-Solutions - Effect of Sodium-Chloride and Humic-Acid. Carbon **32**:93-100.

Benson C. and Trast, J., 1995. Hydraulic Conductivity of Thirteen Compacted Clays. Clays and Clay Minerals **43**: 669-681

Berg, M. et al. 2001. Arsenic contamination of groundwater and drinking water in Vietnam: A human health threat. Environmental Science and Technology **35**: 2621-2626.

Biterna, M., Arditsoglou, A., Tsikouras, E., Voutsa, D., 2007. Arsenate removal by zero valent iron: Batch and column tests. Journal of Hazardous Materials **149**: 548-552.

Blowes, D. W., C. J. Ptacek, and J. L. Jambor. 1997. In-situ remediation of Cr(VI)-contaminated groundwater using permeable reactive walls: Laboratory studies. Environmental Science & Technology **31**:3348-3357.

Bowman, R. 2005. Surfactant-Altered Zeolites as Permeable Barriers for the In-Situ Treatment of Contaminated Groundwater. New Mexico Tech Technical Report 0522. 46 pages.

Bowman, R. 2003. Applications of surfactant-modified zeolites to environmental remediation. Microporous and Mesoporous Materials **61**: 43-56.

Breck, D. 1974. Zeolite Molecular Sieves: Structure, Chemistry and Use. London: John Wiley and Sons, p.4.

Burke, T. et al. 1991. Chromite Ore Processing Residue in Hudson County, New Jersey. Environmental Health Perspectives **92**: 131-137.

California EPA, *Hexavalent Chromium* in Drinking Water California Public Health Goal, July 2011.

Chowdhury, A., Stanforth, R., Overby, R. 2007. Treating Arsenic-Contaminated Soil at a Former Herbicide Blending Facility. Proceedings of the Annual International Conference on soils, sediments, water, and energy. Vol 12.

Chowdhury, S. R. and E. K. Yanful. 2010. Arsenic and chromium removal by mixed magnetite-maghemite nanoparticles and the effect of phosphate on removal. Journal of Environmental Management **91**:2238-2247.

Chowdhury, U. et al. 2000. Groundwater Arsenic contamination in Bangladesh and West Bengal, India. Environmental Health Perspectives, **108**: 393-397.

Chutia, P., Kato, S., Kojima, T., Satokawa, S. Adsorption of As(V) on surfactant-modified natural zeolites. Journal of Hazardous Materials, 162 (2009). 204-211.

Cotton, F. A. 1999. Advanced inorganic chemistry. 6th edition. Wiley, New York.

Davis, M., Lobo R. 1992. Zeolite and Molecular Sieve synthesis. Chem. Mater., **4**: 756-768.

Dhiwar, C., A. Tiwari, and A. K. Bajpai. 2011. Adsorption of Chromium on Composite Microspheres of Chitosan and Nano Iron Oxide. Journal of Dispersion Science and Technology **32**:1661-1667.

Eary, L., Rai, D., 1988. Chromate removal from aqueous waters by reduction with ferrous ion, Environ. Sci. Technol. **22**: 972-977.

EPA. Arsenic Treatment technologies for Soil, Waste and Water. EPA Report 542-R-02-004 (2002).

Farrell, J., Wang, J., O'Day, P., Conklin, M., 2001. Electrochemical and Spectroscopic Study of Arsenate Removal from Water Using Zero-Valent Iron Media. Environ. Sci. Technol. **35**: 2026-2032.

Fay, R. M. and M. M. Mumtaz. 1996. Development of a priority list of chemical mixtures occurring at 1188 hazardous waste sites, using the HazDat database. Food and Chemical Toxicology **34**:1163-1165.

Fruchter, J. 2002. In situ treatment of chromium-contaminated groundwater. Environmental Science & Technology **36**:464a-472a.

Genc, H., Tjell, J., 2003. Effects of phosphate, silicate, sulphate, and bicarbonate on arsenate removal using activated seawater neutralised red mud (bauxsol). Journal de Physique. IV. **107**: 537-540.

Georgiev, D. et al. Synthetic Zeolites – Structure, Classification, Current trends in zeolite synthesis Review. Bulgaria International Science Conference (2009).

Guo, H., Stuben, D., Berner, Z. 2007. Adsorption of arsenic(III) and arsenic(V) from groundwater using natural siderite as the adsorbent. Journal of Colloid Interface Science **315**: 47-53.

Hou, Y. N., H. J. Liu, X. Zhao, J. H. Qu, and J. P. Chen. 2012. Combination of electroreduction with biosorption for enhancement for removal of hexavalent chromium. Journal of Colloid and Interface Science **385**:147-153.

Hristovski, K., et al. 2008. Arsenate removal by Nanostructured ZrO_2 Spheres. Environ. Sci. Technol. **42**: 3786-3790.

Jegadeesan, G., Mondal, K., Lalvani, S., 2005. Arsenate remediation using nanosized modified zerovalent iron particles. Environmental Progress **24**: 289-296.

Kotas, J. and Z. Stasicka. 2000. Chromium occurrence in the environment and methods of its speciation. Environmental Pollution **107**:263-283.

Leyva-Ramos, R., A. Jacobo-Azuara, R. E. Diaz-Flores, R. M. Guerrero-Coronado, J. Mendoza-Barron, and M. S. Berber-Mendoza. 2008. Adsorption of chromium(VI) from an aqueous solution on a surfactant-modified zeolite. Colloids and Surfaces a-Physicochemical and Engineering Aspects **330**:35-41.

Li, G. F., F. Qin, H. Yang, Z. Lu, H. Z. Sun, and R. Chen. 2012. Facile Microwave Synthesis of 3D Flowerlike BiOBr Nanostructures and Their Excellent CrVI Removal Capacity. European Journal of Inorganic Chemistry:2508-2513.

Li, Z. H. 1998. Chromate extraction from surfactant-modified zeolite surfaces. Journal of Environmental Quality **27**:240-242.

Li, Z. H., I. Anghel, and R. S. Bowman. 1998. Sorption of oxyanions by surfactant-modified zeolite. Journal of Dispersion Science and Technology **19**:843-857.

Li, Z. H. and R. S. Bowman. 1998. Sorption of perchloroethylene by surfactant-modified zeolite as controlled by surfactant loading. Environmental Science & Technology **32**:2278-2282.

Li, Z. H. and R. S. Bowman. 2001. Regeneration of surfactant-modified zeolite after saturation with chromate and perchloroethylene. Water Research **35**:322-326.

Li, Z. H., T. Burt, and R. S. Bowman. 2000. Sorption of ionizable organic solutes by surfactant modified zeolite. Environmental Science & Technology **34**:3756-3760.

Li, Z. H., H. K. Jones, P. F. Zhang, and R. S. Bowman. 2007. Chromate transport through columns packed with surfactant-modified zeolite/zero valent iron pellets. Chemosphere **68**:1861-1866.

Liu, Z., et al. 2010. Arsenate removal from water using $Fe_3O_4^-$ loaded activated carbon prepared from waste biomass. Chemical Engineering Journal **160**: 57-62.

Mandal, B., Ogra, Y., and Suzuki, K. 2001. Identification of dimethylarsinous and monomethylarsonous acids in human urine of the arsenic-affected areas in West Bengal, India. Chem. Res. Toxicol. **14**: 371–375.

Melitas, N., et al. 2002. Understanding Soluble Arsenate Removal Kinetics by Zerovalent Iron Media. Environ. Sci. Technol. **36**: 2074-2081.

Mendoza-Barron J., et al. 2011. Adsorption of arsenic(V) from a water solution onto a surfactant-modified zeolite. Adsorption **17**: 489-496.

Min, J. H. and J. G. Hering. 1999. Removal of selenite and chromate using iron(III)-doped alginate gels. Water Environment Research **71**:169-175.

Mohan, D. and C. U. Pittman. 2006. Activated carbons and low cost adsorbents for remediation of tri- and hexavalent chromium from water. Journal of Hazardous Materials **137**:762-811.

Nriagu, J. O. and E. Nieboer. 1988. Chromium in the natural and human environments. Wiley, New York.

Oren, H. and Ozdamar, T., 2013. Hydraulic conductivity of compacted zeolites. Waste Management Res. **31**: 634-640.

Palmer, C. D. and P. R. Wittbrodt. 1991. Processes affecting the remediation of chromium-contaminated sites. Environmental Health Perspectives **92**:25-40.

Pettine, M., Camusso, M. and Martinotti, W., 1992. Dissolved and particulate transport of arsenic and chromium in the Po River, Italy. Sci. Total Environ. **119**: 253–280.

Ponder, S. M., J. G. Darab, and T. E. Mallouk. 2000. Remediation of Cr(VI) and Pb(II) aqueous solutions using supported, nanoscale zero-valent iron. Environmental Science & Technology **34**:2564-2569.

Puls, R., Paul, C., Powell, R. 1999. The application of in situ permeable reactive (zero-valent iron) barrier technology for the remediation of chromate contaminated groundwater: a field test. Appl. Geochem. **14**: 989-1000.

Ranck, M., et al. 2005. BTEX Removal from Produced Water Using Surfactant Modified Zeolite. Journal of Environmental Engineering **131**: 434-442.

Rasouli, M., N. Yaghobi, M. Hafezi, and M. Rasouli. 2012. Adsorption of divalent lead ions from aqueous solution using low silica nano-zeolite X. Journal of Industrial and Engineering Chemistry **18**:1970-1976.

Saada, A., Breeze, D., Crouzet, C., Cornu, S., Baranger, P. 2003. Adsorption of arsenic (V) on kaolinite and on kaolinite-humic acid complexes: role of humic acid nitrogen groups. Chemosphere **51**: 757-763.

Salem, A., H. Afshin, and H. Behsaz. 2012. Removal of lead by using Raschig rings manufactured with mixture of cement kiln dust, zeolite and bentonite. Journal of Hazardous Materials **223**:13-23.

Schick, J., P. Caullet, J. L. Paillaud, J. Patarin, S. Freitag, and C. Mangold-Callarec. 2012. Phosphate uptake from water on a Surfactant-Modified Zeolite and Ca-zeolites. Journal of Porous Materials **19**:405-414.

Sharma, Y. C., V. Srivastava, and A. K. Mukherjee. 2010. Synthesis and Application of Nano-Al2O3 Powder for the Reclamation of Hexavalent Chromium from Aqueous Solutions. Journal of Chemical and Engineering Data **55**:2390-2398.

Schulze-Makuch, D., Bowman, R., Pillai, S., Guan, H. 2003. Field Evaluation of the Effectiveness of Surfactant Modified Zeolite and Iron-Oxide-Coated Sand for Removing Viruses and Bacteria from Ground Water. Ground Water Monitoring and Remediation **23**: 68-75.

Schulze-Makuch, D., Bowman, R., Pillai, S. 2003. Removal of biological pathogens using surfactant-modified zeolite. Patent 07311839.

Schulze-Makuch, D. et al. 2002. Surfactant-modified zeolite can protect drinking water wells from viruses and bacteria. EOS Transactions, American Geophysical Union 83 no.**18**: 193-204.

Sharma, P., Bihari, V., Agarwal, S., Goel, S., 2012. Genetic Predisposition for Dermal Problems in Hexavalent chromium Exposed Population. Journal of Nucleic Acids **2012**: 9 pages.

Shi, L. N., Y. M. Lin, X. Zhang, and Z. L. Chen. 2011. Synthesis, characterization and kinetics of bentonite supported nZVI for the removal of Cr(VI) from aqueous solution. Chemical Engineering Journal **171**:612-617.

Shinzato, M. C., T. J. Montanheiro, V. A. Janasi, S. Andrade, and J. K. Yamamoto. 2012. Removal of Pb2+ from aqueous solutions using two Brazilian rocks containing zeolites. Environmental Earth Sciences **66**:363-370.

Smedley, P. and Kinniburgh, D., 2002. A review of the source, behaviour and distribution of arsenic in natural waters. Appl. Geochem. **17**: 517–568.

Smith, A., Lingas, E., and Rahman, M. 2000. Contamination of drinking-water by arsenic in Bangladesh: a public health emergency. Bulletin of the World Health Organization 9.

St. Cloud Mining Company. What is Zeolite? (2012). http://www.stcloudmining.com/what-is-zeolite.html accessed 2/12/2013.

Stevik, T. et al. 2004. Retention and removal of pathogenic bacteria in wastewater percolation through porous media: a review. Water Research **38**: 1355-1367.

Swarnkar V., Agrawal N., Tomar, R. 2011. Sorption of chromate by HDTMA-Exchanged Zeolites. Journal of Chemical and Pharmaceutical Research, **3**: 520-529.

Tandon, R. K., P. T. Crisp, J. Ellis, and R. S. Baker. 1984. Effect of pH on chromium(VI) species in solution. Talanta **31**:227-228.

Terlecka, E., 2005. Arsenic Speciation Analysis in Water Samples: A Review of the Hyphenated Techniques. Environmental Monitoring and Assessment **107**: 259-284.

Tokyo Metropolitan Government Bureau of Sanitation. Survey of Health Effects from Chromium Contamination: Fourth Report. Tokyo, Japan, March, 1987.

United Nations Synthesis Report on Arsenic in Drinking Water, 2001.

Vitra, R. Natural and Synthetic Zeolites. Geotimes (2008).

Xu, S. P. and P. R. Jaffe. 2006. Effects of plants on the removal of hexavalent chromium in wetland sediments. Journal of Environmental Quality **35**:334-341.

Yusof, A., Malek, N. 2009. Removal of Cr(VI) and As(V) from aqueous solutions by HDTMA-modified zeolite Y. Journal of Hazardous Materials **162**: 1019-1024.

Zeng, Y., Woo, H., Lee, G., Park, J. 2010. Removal of chromate from water using surfactant modified Pohnag clinoptilolite and Haruna chabazite. Desalination **257**: 102-109.

Zhang, K., et al, 2010. Graphene oxide/ferric hydroxide composites for efficient arsenate removal from drinking water. Journal of Hazardous Materials **182**: 162-168.

Zhang, Q., et al, 2008. Arsenate removal from Aqueous Media by Nanosized Hydrated Ferric Oxide (HFO)-Loaded Polymeric Sorbents: Effect of HFO Loadings. Industrial and Engineering Chemistry Research **47**: 3957-3962.

Zhang, S., et al., 2008. Arsenate removal from aqueous solutions using modified red mud. Journal of Hazardous Materials **152**: 486-492.

Zhao, Y. G., H. Y. Shen, S. D. Pan, M. Q. Hu, and Q. H. Xia. 2010. Preparation and characterization of amino-functionalized nano-Fe3O4 magnetic polymer adsorbents for removal of chromium(VI) ions. Journal of Materials Science **45**:5291-5301.

APPENDIX A

KINETICS DATA FOR CHROMATE AT VARYING pH AND IONIC STRENGTH

Table A.1. Kinetics batch experiment data for pH 7 and ionic strength 5mM for sample set 1. Final concentration of chromate was calculated from calibration curve data by the following equation: Abs. = (0.321904*final conc.)-0.013

Sample Set 2 Kinetics pH 7, ionic stength 5mM			
Time (min)	Abs @ 540nm (2)	Final Conc. mg/L (2)	Conc. Absorbed on zeolite mM/kg (2)
0	0.5547	171.018	0.000
2	0.3627	111.373	11.472
15	0.299	91.585	15.279
30	0.2922	89.472	15.685
60	0.2814	86.117	16.330
150	0.2611	79.811	17.543
300	0.267	81.644	17.191
1440	0.2339	71.361	19.169

Table A.2. Kinetics batch experiment data for pH 7 and ionic strength 5mM for sample set 2. Final concentration of chromate was calculated from calibration curve data by the following equation: Abs. = (0.321904*final conc.)-0.013

Sample Set 2 Kinetics pH 7, ionic stength 5mM			
Time (min)	Abs @ 540nm (2)	Final Conc. mg/L (2)	Conc. Absorbed on zeolite mM/kg (2)
0	0.5615	173.131	0.000
2	0.349	107.117	12.697
15	0.2914	89.224	16.139
30	0.2905	88.944	16.193
60	0.2804	85.807	16.796
150	0.2561	78.258	18.248
300	0.2522	77.046	18.481
1440	0.2435	74.344	19.001

Table A.3. Kinetics batch experiment data for pH 7 and ionic strength 20mM for sample set 1. Final concentration of chromate was calculated from calibration curve data by the following equation: Abs. = (0.321904*final conc.)-0.013

Sample Set 1 Kinetics pH 7, ionic stength 20mM			
Time (min)	Abs @ 540nm (1)	Final Conc. mg/L (1)	Conc. Absorbed on zeolite mM/kg (1)
0	0.5523	170.273	0.000
2	0.4214	129.609	7.822
5	0.3962	121.780	9.327
15	0.3749	115.163	10.600
30	0.3721	114.293	10.767
60	0.3641	111.808	11.245
150	0.3693	113.424	10.935
1440	0.3418	104.881	12.578

Table A.4. Kinetics batch experiment data for pH 7 and ionic strength 20mM for sample set 2. Final concentration of chromate was calculated from calibration curve data by the following equation: Abs. = (0.321904*final conc.)-0.013

Sample Set 2 Kinetics pH 7, ionic stength 20mM			
Time (min)	Abs @ 540nm (2)	Final Conc. mg/L (2)	Conc. Absorbed on zeolite mM/kg (2)
0	0.5493	169.341	0.000
2	0.4144	127.434	8.061
15	0.3744	115.008	10.451
60	0.355	108.981	11.610
150	0.3453	105.968	12.189
300	0.3458	106.123	12.160
1440	0.3508	107.677	11.861

Table A.5. Kinetics batch experiment data for pH 7 and ionic strength 100mM for sample set 1. Final concentration of chromate was calculated from calibration curve data by the following equation: Abs. = (0.321904*final conc.)-0.013

Sample Set 1 Kinetics pH 7, ionic stength 100mM			
Time (min)	Abs @ 540nm (1)	Final Conc. mg/L (1)	Conc. Absorbed on zeolite mM/kg (1)
0	0.5342	164.650	0.000
2	0.501	154.336	1.984
15	0.4862	149.739	2.868
150	0.4738	145.887	3.609
300	0.4766	146.757	3.442
1440	0.4812	148.186	3.167

Table A.6. Kinetics batch experiment data for pH 7 and ionic strength 100mM for sample set 2. Final concentration of chromate was calculated from calibration curve data by the following equation: Abs. = (0.321904*final conc.)-0.013

Sample Set 2 Kinetics pH 7, ionic stength 100mM			
Time (min)	Abs @ 540nm (2)	Final Conc. mg/L (2)	Conc. Absorbed on zeolite mM/kg (2)
0	0.5354	165.023	0.000
2	0.4891	150.640	2.766
15	0.4849	149.335	3.017
150	0.4668	143.712	4.099
300	0.4719	145.297	3.794
1440	0.4705	144.862	3.878

Table A.7. Kinetics batch experiment data for pH 9 and ionic strength 20mM for sample set 1. Final concentration of chromate was calculated from calibration curve data by the following equation: Abs. = (0.321904*final conc.)-0.013

Sample Set 1 Kinetics pH 9, ionic stength 20mM			
Time (min)	Abs @ 540nm (1)	Final Conc. mg/L (1)	Conc. Absorbed on zeolite mM/kg (1)
0	0.5515	170.024	0.000
2	0.4689	144.365	4.935
5	0.403	123.893	8.873
15	0.3822	117.431	10.116
30	0.3622	111.218	11.311
60	0.3438	105.502	12.410
150	0.3574	109.727	11.598
300	0.3383	103.793	12.739
1440	0.293	89.721	15.446

Table A.8. Kinetics batch experiment data for pH 9 and ionic strength 20mM for sample set 2. Final concentration of chromate was calculated from calibration curve data by the following equation: Abs. = (0.321904*final conc.)-0.013

Sample Set 2 Kinetics pH 9, ionic stength 20mM			
Time (min)	Abs @ 540nm (2)	Final Conc. mg/L (2)	Conc. Absorbed on zeolite mM/kg (2)
0	0.5515	170.024	0.000
2	0.4597	141.507	5.485
5	0.4049	124.483	8.759
15	0.3821	117.400	10.122
30	0.3732	114.635	10.654
60	0.3641	111.808	11.197
150	0.3597	110.441	11.460
300	0.319	97.798	13.892
1440	0.3074	94.194	14.585

Table A.9. Kinetics batch experiment data for pH 4 and ionic strength 20mM for sample set 1. Final concentration of chromate was calculated from calibration curve data by the following equation: Abs. = (0.321904*final conc.)-0.013

Sample Set 1 Kinetics pH 4, ionic stength 20mM			
Time (min)	Abs @ 540nm (1)	Final Conc. mg/L (1)	Conc. Absorbed on zeolite mM/kg (1)
0	0.5735	176.859	0.000
2	0.4038	124.141	10.140
15	0.3699	113.610	12.165
60	0.3641	111.808	12.512
150	0.3525	108.205	13.205
300	0.3539	108.640	13.121
1440	0.343	105.254	13.773

Table A.10. Kinetics batch experiment data for pH 4 and ionic strength 20mM for sample set 2. Final concentration of chromate was calculated from calibration curve data by the following equation: Abs. = (0.321904*final conc.)-0.013

Sample Set 2 Kinetics pH 4, ionic stength 20mM			
Time (min)	Abs @ 540nm (2)	Final Conc. mg/L (2)	Conc. Absorbed on zeolite mM/kg (2)
0	0.5677	175.057	0.000
2	0.4008	123.209	9.972
15	0.3605	110.690	12.380
60	0.3469	106.465	13.193
150	0.3508	107.677	12.960
300	0.3383	103.793	13.707
1440	0.3297	101.122	14.221

APPENDIX B

BATCH EXPERIMENT DATA FOR CHROMATE AT VARYING pH AND IONIC STRENGTH

Table B.1. Batch experiment data for pH 4 and ionic strength 5mM for sample set 1. Final concentration of chromate was calculated from calibration curve data by the following equation: Abs. = (0.321904*final conc.)-0.013

Sample Set 1 Batch experiments pH 4, ionic stength 5mM				
Original Conc. (mg/L)	Abs @ 540nm (1)	Final Conc. mg/L (1)	Final Conc mM (1)	Conc. Absorbed on zeolite mM/kg (1)
0	0	0.000	0.000	0.000
5	0.0067	0.078	0.002	0.947
10	0.0157	0.358	0.007	1.854
25	0.0452	1.274	0.025	4.563
50	0.0182	2.177	0.042	9.197
75	0.1053	15.706	0.302	11.404
100	0.1428	21.531	0.414	15.091
125	0.1064	31.753	0.611	17.933
150	0.1877	57.009	1.096	17.884
200	0.2798	85.620	1.647	21.998
250	0.4059	124.793	2.400	24.080
300	0.2712	165.897	3.191	25.791
500	0.5756	355.022	6.828	27.883
600	0.4987	460.866	8.863	26.759
750	0.6504	602.243	11.582	28.417

Table B.2. Batch experiment data for pH 4 and ionic strength 5mM for sample set 2. Final concentration of chromate was calculated from calibration curve data by the following equation: Abs. = (0.321904*final conc.)-0.013

Sample Set 2 Batch experiments pH 4, ionic stength 5mM				
Original Conc. (mg/L)	Abs @ 540nm (2)	Final Conc. mg/L (2)	Final Conc mM (2)	Conc. Absorbed on zeolite mM/kg (2)
0	0	0.000	0.000	0.000
5	0.0054	0.038	0.001	0.954
10	0.012	0.243	0.005	1.877
25	0.0509	1.451	0.028	4.529
50	0.041	5.718	0.110	8.516
75	0.0986	14.665	0.282	11.604
100	0.1279	19.216	0.370	15.537
125	0.1288	38.712	0.745	16.595
150	0.1692	51.262	0.986	18.989
200	0.2786	85.248	1.640	22.069
250	0.452	139.115	2.675	21.326
300	0.2618	160.057	3.078	26.914
500	0.5824	359.247	6.909	27.070
600	0.4907	453.410	8.720	28.193
750	0.6573	608.674	11.706	27.180

Table B.3. Batch experiment data for pH 4 and ionic strength 20mM for sample set 1. Final concentration of chromate was calculated from calibration curve data by the following equation: Abs. = (0.321904*final conc.)-0.013

Sample Set 1 Batch experiments pH 4, ionic stength 20mM				
Original Conc. (mg/L)	Abs @ 540nm (1)	Final Conc. mg/L (1)	Final Conc mM (1)	Conc. Absorbed on zeolite mM/kg (1)
0	0	0.000	0.000	0.000
5	0.0309	0.830	0.016	0.802
10	0.0723	2.116	0.041	1.516
25	0.2018	6.139	0.118	3.627
50	0.1025	15.271	0.294	6.679
75	0.1906	28.955	0.557	8.855
100	0.259	39.579	0.761	11.620
125	0.1984	60.333	1.160	12.437
150	0.2424	74.002	1.423	14.616
200	0.3555	109.137	2.099	17.475
300	0.3285	201.498	3.875	18.944
500	0.6497	401.061	7.713	19.028
600	0.5414	500.660	9.629	19.105
750	0.6907	639.801	12.305	21.194

Table B.4. Batch experiment data for pH 4 and ionic strength 20mM for sample set 2. Final concentration of chromate was calculated from calibration curve data by the following equation: Abs. = (0.321904*final conc.)-0.013

Sample Set 2 Batch experiments pH 4, ionic stength 20mM				
Original Conc. (mg/L)	Abs @ 540nm (2)	Final Conc. mg/L (2)	Final Conc mM (2)	Conc. Absorbed on zeolite mM/kg (2)
0	0	0.000	0.000	0.000
5	0.0365	0.830	0.019	0.769
10	0.0802	2.116	0.045	1.469
25	0.2057	6.139	0.120	3.604
50	0.1084	15.271	0.311	6.503
75	0.1752	28.955	0.511	9.316
100	0.2555	39.579	0.751	11.725
125	0.1899	60.333	1.110	12.945
150	0.2249	74.002	1.319	15.662
200	0.371	109.137	2.192	16.549
300	0.3257	201.498	3.842	19.279
500	0.6281	401.061	7.455	21.609
600	0.53	500.660	9.424	21.149
750	0.6735	639.801	11.997	24.277

Table B.5. Batch experiment data for pH 4 and ionic strength 100mM for sample set 1. Final concentration of chromate was calculated from calibration curve data by the following equation: Abs. = (0.321904*final conc.)-0.013

Sample Set 1 Batch experiments pH 4, ionic stength 100mM				
Original Conc. (mg/L)	Abs @ 540nm (1)	Final Conc. mg/L (1)	Final Conc mM (1)	Conc. Absorbed on zeolite mM/kg (1)
0	0	0.000	0.000	0.000
5	0.1205	3.613	0.069	0.267
10	0.2346	7.158	0.138	0.547
25	0.5656	17.440	0.335	1.454
50	0.2495	38.104	0.733	2.288
75	0.3566	54.739	1.053	3.897
100	0.4945	76.159	1.465	4.585
125	0.3079	94.350	1.815	5.895
150	0.3663	112.492	2.163	7.214
200	0.4946	152.348	2.930	9.164
250	0.6384	197.020	3.789	10.189
300	0.4625	284.753	5.476	12.549
500	0.6659	411.126	7.907	17.093

Table B.6. Batch experiment data for pH 4 and ionic strength 100mM for sample set 2. Final concentration of chromate was calculated from calibration curve data by the following equation: Abs. = (0.321904*final conc.)-0.013

Sample Set 2 Batch experiments pH 4, ionic stength 100mM				
Original Conc. (mg/L)	Abs @ 540nm (2)	Final Conc. mg/L (2)	Final Conc mM (2)	Conc. Absorbed on zeolite mM/kg (2)
0	0	0.000	0.000	0.000
5	0.1179	3.533	0.068	0.282
10	0.2452	7.487	0.144	0.483
25	0.5997	18.500	0.356	1.250
50	0.2488	37.995	0.731	2.309
75	0.3645	55.966	1.076	3.661
100	0.505	77.790	1.496	4.272
125	0.3239	99.320	1.910	4.939
150	0.3843	118.083	2.271	6.138
200	0.5165	159.152	3.061	7.856
250	0.6534	201.680	3.879	9.293
300	0.4606	283.572	5.454	12.776
500	0.6738	416.034	8.001	16.149

Table B.7. Batch experiment data for pH 7 and ionic strength 5mM for sample set 1. Final concentration of chromate was calculated from calibration curve data by the following equation: Abs. = (0.321904*final conc.)-0.013

Sample Set 1 Batch experiments pH 7, ionic stength 5mM				
Original Conc. (mg/L)	Abs @ 540nm (1)	Final Conc. mg/L (1)	Final Conc mM (1)	Conc. Absorbed on zeolite mM/kg (1)
0	0	0.000	0.000	0.000
5	0.0032	-0.031	-0.001	0.967
10	0.0122	0.249	0.005	1.875
25	0.0409	1.141	0.022	4.589
50	0.0313	4.212	0.081	8.806
75	0.0673	9.803	0.189	12.539
100	0.1461	22.043	0.424	14.993
125	0.1061	31.660	0.609	17.951
150	0.172	52.132	1.003	18.822
200	0.3014	92.330	1.776	20.707
250	0.4072	125.197	2.408	24.002
300	0.2916	178.572	3.434	23.353
500	0.5791	357.197	6.870	27.464
600	0.5032	465.060	8.944	25.952
750	0.6787	628.618	12.090	23.345

Table B.8. Batch experiment data for pH 7 and ionic strength 5mM for sample set 2. Final concentration of chromate was calculated from calibration curve data by the following equation: Abs. = (0.321904*final conc.)-0.013

Sample Set 2 Batch experiments pH 7, ionic stength 5mM				
Original Conc. (mg/L)	Abs @ 540nm (2)	Final Conc. mg/L (2)	Final Conc mM (2)	Conc. Absorbed on zeolite mM/kg (2)
0	0	0.000	0.000	0.000
5	0.0038	-0.012	0.000	0.964
10	0.016	0.367	0.007	1.853
25	0.0444	1.249	0.024	4.568
50	0.0472	6.681	0.128	8.331
75	0.0818	12.056	0.232	12.106
100	0.1223	18.346	0.353	15.704
125	0.1293	38.867	0.748	16.565
150	0.1713	51.915	0.998	18.864
200	0.2684	82.079	1.579	22.679
250	0.4419	135.977	2.615	21.929
300	0.2739	167.575	3.223	25.468
500	0.5985	369.250	7.102	25.146
600	0.4991	461.239	8.871	26.687

Table B.9. Batch experiment data for pH 7 and ionic strength 20mM for sample set 1. Final concentration of chromate was calculated from calibration curve data by the following equation: Abs. = (0.321904*final conc.)-0.013

Sample Set 1 Batch experiments pH 7, ionic stength 20mM				
Original Conc. (mg/L)	Abs @ 540nm (1)	Final Conc. mg/L (1)	Final Conc mM (1)	Conc. Absorbed on zeolite mM/kg (1)
0	0	0.000	0.000	0.000
5	0.0262	0.684	0.013	0.830
10	0.0537	1.538	0.030	1.627
25	0.1779	5.396	0.104	3.770
50	0.0897	13.283	0.255	7.062
75	0.1962	29.825	0.574	8.688
125	0.1859	56.450	1.086	13.184
150	0.2294	69.963	1.346	15.393
200	0.3562	109.354	2.103	17.433
300	0.3353	205.723	3.957	18.132
500	0.6196	382.359	7.354	22.625
600	0.5208	481.462	9.260	22.798
750	0.6801	629.923	12.115	23.094

Table B.10. Batch experiment data for pH 7 and ionic strength 20mM for sample set 2. Final concentration of chromate was calculated from calibration curve data by the following equation: Abs. = (0.321904*final conc.)-0.013

Sample Set 2 Batch experiments pH 7, ionic stength 20mM				
Original Conc. (mg/L)	Abs @ 540nm (2)	Final Conc. mg/L (2)	Final Conc mM (2)	Conc. Absorbed on zeolite mM/kg (2)
0	0	0.000	0.000	0.000
5	0.0259	0.675	0.013	0.832
10	0.0581	1.675	0.032	1.601
25	0.1803	5.471	0.105	3.756
50	0.1036	15.442	0.297	6.646
75	0.1782	27.029	0.520	9.226
125	0.1947	59.184	1.138	12.658
150	0.2212	67.416	1.297	15.883
200	0.356	109.292	2.102	17.445
300	0.3326	204.045	3.924	18.454
500	0.6039	372.605	7.166	24.501
600	0.5318	491.714	9.457	20.826
750	0.6963	645.020	12.405	20.190

Table B.11. Batch experiment data for pH 7 and ionic strength 100mM for sample set 1. Final concentration of chromate was calculated from calibration curve data by the following equation: Abs. = (0.321904*final conc.)-0.013

Sample Set 1 Batch experiments pH 7, ionic stength 100mM				
Original Conc. (mg/L)	Abs @ 540nm (1)	Final Conc. mg/L (1)	Final Conc mM (1)	Conc. Absorbed on zeolite mM/kg (1)
0	0	0.000	0.000	0.000
5	0.1198	3.592	0.069	0.271
10	0.2512	7.674	0.148	0.447
25	0.6724	20.758	0.399	0.816
50	0.2561	39.129	0.753	2.091
75	0.3905	60.005	1.154	2.884
100	0.5071	78.116	1.502	4.209
125	0.3308	101.464	1.951	4.527
150	0.4066	125.011	2.404	4.806
200	0.5392	166.203	3.196	6.500
250	0.6724	207.582	3.992	8.158
300	0.4901	301.901	5.806	9.251
500	0.6531	403.173	7.754	18.622
600	0.5217	482.301	9.276	22.636

Table B.12. Batch experiment data for pH 7 and ionic strength 100mM for sample set 2. Final concentration of chromate was calculated from calibration curve data by the following equation: Abs. = (0.321904*final conc.)-0.013

Sample Set 2 Batch experiments pH 7, ionic stength 100mM				
Original Conc. (mg/L)	Abs @ 540nm (2)	Final Conc. mg/L (2)	Final Conc mM (2)	Conc. Absorbed on zeolite mM/kg (2)
0	0	0.000	0.000	0.000
5	0.1205	3.613	0.069	0.267
10	0.2631	8.043	0.155	0.376
25	0.6843	21.128	0.406	0.745
50	0.2605	39.812	0.766	1.959
75	0.3964	60.921	1.172	2.708
100	0.5018	77.292	1.487	4.367
125	0.3398	104.259	2.005	3.989
150	0.3923	120.569	2.319	5.660
200	0.5347	164.805	3.170	6.769
250	0.678	209.322	4.026	7.823
300	0.4829	297.427	5.720	10.111
500	0.6675	412.120	7.926	16.901
600	0.5115	472.795	9.093	24.464

Table B.13. Batch experiment data for pH 9 and ionic strength 5mM for sample set 1. Final concentration of chromate was calculated from calibration curve data by the following equation: Abs. = (0.321904*final conc.)-0.013

Sample Set 1 Batch experiments pH 9, ionic stength 5mM				
Original Conc. (mg/L)	Abs @ 540nm (1)	Final Conc. mg/L (1)	Final Conc mM (1)	Conc. Absorbed on zeolite mM/kg (1)
0	0	0.000	0.000	0.000
5	0.0056	0.044	0.001	0.953
10	0.0148	0.330	0.006	1.860
25	0.0424	1.187	0.023	4.580
50	0.0237	3.031	0.058	9.033
75	0.0706	10.316	0.198	12.440
100	0.1173	17.570	0.338	15.853
125	0.0889	26.317	0.506	18.979
150	0.1012	30.138	0.580	23.052
200	0.2493	76.145	1.464	23.820
250	0.3203	98.202	1.889	29.194
300	0.2539	155.149	2.984	27.858
500	0.5503	339.303	6.526	30.906
600	0.475	438.779	8.439	31.007
750	0.6284	581.740	11.188	32.360

Table B.14. Batch experiment data for pH 9 and ionic strength 5mM for sample set 2. Final concentration of chromate was calculated from calibration curve data by the following equation: Abs. = (0.321904*final conc.)-0.013

Sample Set 2 Batch experiments pH 9, ionic stength 5mM				
Original Conc. (mg/L)	Abs @ 540nm (2)	Final Conc. mg/L (2)	Final Conc mM (2)	Conc. Absorbed on zeolite mM/kg (2)
0	0	0.000	0.000	0.000
5	0.006	0.056	0.001	0.951
10	0.0143	0.314	0.006	1.863
25	0.0479	1.358	0.026	4.547
50	0.0277	3.653	0.070	8.914
75	0.0624	9.042	0.174	12.685
100	0.1284	19.294	0.371	15.522
125	0.0891	26.379	0.507	18.967
150	0.1343	40.421	0.777	21.075
200	0.2189	66.702	1.283	25.636
250	0.3489	107.086	2.060	27.486
300	0.2638	161.300	3.102	26.675
500	0.5529	340.919	6.557	30.595
600	0.4663	430.671	8.283	32.566
750	0.6425	594.881	11.441	29.833

Table B.15. Batch experiment data for pH 9 and ionic strength 20mM for sample set 1. Final concentration of chromate was calculated from calibration curve data by the following equation: Abs. = (0.321904*final conc.)-0.013

Sample Set 1 Batch experiments pH 9, ionic stength 20mM				
Original Conc. (mg/L)	Abs @ 540nm (1)	Final Conc. mg/L (1)	Final Conc mM (1)	Conc. Absorbed on zeolite mM/kg (1)
0	0	0.000	0.000	0.000
5	0.035	0.957	0.018	0.778
10	0.0741	2.172	0.042	1.506
25	0.2402	7.332	0.141	3.398
50	0.0922	13.671	0.263	6.987
75	0.1777	26.951	0.518	9.241
100	0.2697	41.241	0.793	11.301
125	0.1753	53.157	1.022	13.817
150	0.2382	72.697	1.398	14.867
200	0.3427	105.160	2.022	18.240
250	0.4634	142.656	2.744	20.645
300	0.3091	189.445	3.643	21.262
500	0.6025	371.735	7.149	24.668
600	0.5245	484.910	9.326	22.134
750	0.6707	621.162	11.946	24.778

Table B.16. Batch experiment data for pH 9 and ionic strength 20mM for sample set 2. Final concentration of chromate was calculated from calibration curve data by the following equation: Abs. = (0.321904*final conc.)-0.013

Sample Set 2 Batch experiments pH 9, ionic stength 20mM				
Original Conc. (mg/L)	Abs @ 540nm (2)	Final Conc. mg/L (2)	Final Conc mM (2)	Conc. Absorbed on zeolite mM/kg (2)
0	0	0.000	0.000	0.000
5	0.0338	0.920	0.018	0.785
10	0.0801	2.358	0.045	1.470
25	0.2222	6.773	0.130	3.506
50	0.1051	15.675	0.301	6.602
75	0.1924	29.235	0.562	8.802
100	0.2883	44.130	0.849	10.745
125	0.1777	53.903	1.037	13.674
150	0.2274	69.342	1.334	15.512
200	0.3502	107.490	2.067	17.792
250	0.4828	148.683	2.860	19.486
300	0.3171	194.415	3.739	20.306
500	0.6079	375.090	7.214	24.023
600	0.5103	471.677	9.071	24.679
750	0.667	617.714	11.880	25.442

Table B.17. Batch experiment data for pH 9 and ionic strength 100mM for sample set 1. Final concentration of chromate was calculated from calibration curve data by the following equation: Abs. = (0.321904*final conc.)-0.013

Sample Set 1 Batch experiments pH 9, ionic stength 100mM				
Original Conc. (mg/L)	Abs @ 540nm (1)	Final Conc. mg/L (1)	Final Conc mM (1)	Conc. Absorbed on zeolite mM/kg (1)
0	0	0.000	0.000	0.000
5	0.1184	3.548	0.068	0.279
10	0.2324	7.090	0.136	0.560
25	0.6008	18.534	0.356	1.244
50	0.2395	36.551	0.703	2.587
75	0.3621	55.593	1.069	3.732
100	0.4608	70.924	1.364	5.592
125	0.2848	87.174	1.677	7.275
150	0.3525	108.205	2.081	8.038
200	0.4792	147.564	2.838	10.085
250	0.5796	178.754	3.438	13.702
300	0.411	252.756	4.861	18.702
500	0.606	373.910	7.191	24.250
600	0.5386	498.051	9.579	19.607
850	0.7524	697.303	13.411	29.367

Table B.18. Batch experiment data for pH 9 and ionic strength 100mM for sample set 2. Final concentration of chromate was calculated from calibration curve data by the following equation: Abs. = (0.321904*final conc.)-0.013

Sample Set 2 Batch experiments pH 9, ionic stength 100mM				
Original Conc. (mg/L)	Abs @ 540nm (2)	Final Conc. mg/L (2)	Final Conc mM (2)	Conc. Absorbed on zeolite mM/kg (2)
0	0	0.000	0.000	0.000
5	0.113	3.380	0.065	0.311
10	0.2404	7.338	0.141	0.512
25	0.6017	18.562	0.357	1.238
50	0.2285	34.842	0.670	2.915
75	0.3574	54.863	1.055	3.873
100	0.4647	71.530	1.376	5.475
125	0.2887	88.385	1.700	7.042
150	0.3549	108.950	2.095	7.895
200	0.4619	142.190	2.735	11.118
250	0.5922	182.668	3.513	12.949
300	0.4298	264.436	5.086	16.456
500	0.5917	365.025	7.020	25.959
600	0.4924	454.995	8.751	27.888
750	0.7855	728.151	14.004	23.434

APPENDIX C

KINETICS DATA FOR ARSENATE AT DIFFERENT pH AND IONIC STRENGTH CONDITIONS

Table C.1. Kinetics batch experiment data for pH 7 and ionic strength 1mM for sample set 1. Final concentration of arsenate was calculated from calibration curve data from AAS.

Sample Set 1 Kinetics pH 7, ionic stength 1mM			
Time (min)	Abs. (1)	Final Conc. mg/L (1)	Conc. Absorbed on zeolite mM/kg (1)
0	0.364	148.41	0.00
1	0.277	107.22	5.50
2	0.254	97.54	6.79
5	0.242	91.42	7.61
15	0.233	87.59	8.12
30	0.239	90.18	7.77
60	0.236	88.7	7.97
120	0.241	91	7.66
240	0.239	89.98	7.80
1320	0.239	83.19	8.71
1440	0.233	87.29	8.16

Table C.2. Kinetics batch experiment data for pH 7 and ionic strength 1mM for sample set 2. Final concentration of arsenate was calculated from calibration curve data from AAS.

Sample Set 2 Kinetics pH 7, ionic stength 1mM			
Time (min)	Abs. (2)	Final Conc. mg/L (2)	Conc. Absorbed on zeolite mM/kg (2)
0	0.364	148.41	0.00
1	0.277	106.17	5.64
2	0.227	84.36	8.55
5	0.247	94.16	7.24
15	0.237	89.17	7.91
30	0.239	90.17	7.77
60	0.235	88.37	8.01
120	0.24	90.24	7.76
240	0.239	90.04	7.79
1320	0.224	87.31	8.16
1440	0.239	89.49	7.86

Table C.3. Kinetics batch experiment data for pH 7 and ionic strength 5mM for sample set 1. Final concentration of arsenate was calculated from calibration curve data from AAS.

Sample Set 1 Kinetics pH 7, ionic stength 5mM			
Time (min)	Abs. (1)	Final Conc. mg/L (1)	Conc. Absorbed on zeolite mM/kg (1)
0	0.559	143.18	0.00
1	0.545	99.95	5.77
2	0.426	105.73	5.00
5	0.446	103.58	5.29
15	0.439	97.38	6.11
30	0.414	99.00	5.90
60	0.083	99.72	5.80
120	0.082	98.54	5.96
240	0.084	101.68	5.54
1320	0.081	97.82	6.05
1440	0.081	96.82	6.19

Table C.4. Kinetics batch experiment data for pH 7 and ionic strength 5mM for sample set 2. Final concentration of arsenate was calculated from calibration curve data from AAS.

Sample Set 2 Kinetics pH 7, ionic stength 5mM			
Time (min)	Abs. (2)	Final Conc. mg/L (2)	Conc. Absorbed on zeolite mM/kg (2)
0	0.668	147.93	0.00
1	0.555	106.40	5.54
2	0.449	102.49	6.07
5	0.436	98.93	6.54
15	0.421	98.61	6.58
30	0.42	97.42	6.74
60	0.08	100.46	6.34
120	0.085	99.08	6.52
240	0.082	99.40	6.48
1320	0.08	101.07	6.25
1440	0.079	106.63	5.51

Table C.5. Kinetics batch experiment data for pH 7 and ionic strength 20mM for sample set 1. Final concentration of arsenate was calculated from calibration curve data from AAS.

Sample Set 1 Kinetics pH 7, ionic stength 20mM			
Time (min)	Abs. (1)	Final Conc. mg/L (1)	Conc. Absorbed on zeolite mM/kg (1)
0	0.55	151.72	0.00
1	0.504	136.08	2.09
2	0.502	135.37	2.18
5	0.506	136.49	2.03
15	0.502	135.22	2.20
30	0.5	134.79	2.26
60	0.484	129.30	2.99
120	0.493	132.42	2.58
240	0.494	132.60	2.55
1320	0.473	125.64	3.48
1440	0.498	133.92	2.38

Table C.6. Kinetics batch experiment data for pH 7 and ionic strength 20mM for sample set 2. Final concentration of arsenate was calculated from calibration curve data from AAS.

Sample Set 2 Kinetics pH 7, ionic stength 20mM			
Time (min)	Abs. (2)	Final Conc. mg/L (2)	Conc. Absorbed on zeolite mM/kg (2)
0	0.54	148.11	0.00
1	0.507	139.95	1.09
2	0.52	141.39	0.90
5	0.492	131.93	2.16
15	0.48	127.81	2.71
30	0.483	128.77	2.58
60	0.491	131.72	2.19
120	0.495	132.87	2.03
240	0.486	130.05	2.41
1320	0.498	133.94	1.89
1440	0.514	139.44	1.16

Table C.7. Kinetics batch experiment data for pH 4 and ionic strength 20mM for sample set 1. Final concentration of arsenate was calculated from calibration curve data from AAS.

Sample Set 1 Kinetics pH 4, ionic stength 20mM			
Time (min)	Abs. (1)	Final Conc. mg/L (1)	Conc. Absorbed on zeolite mM/kg (1)
0	0.5	145.24	0.00
1	0.458	128.62	2.22
2	0.451	125.63	2.62
5	0.449	124.78	2.73
15	0.448	124.45	2.78
30	0.441	122.19	3.08
60	0.438	121.32	3.19
120	0.432	119.35	3.46
240	0.434	119.76	3.40
1320	0.432	119.06	3.49

Table C.8. Kinetics batch experiment data for pH 4 and ionic strength 5mM for sample set 2. Final concentration of arsenate was calculated from calibration curve data from AAS.

Sample Set 2 Kinetics pH 4, ionic stength 20mM			
Time (min)	Abs. (2)	Final Conc. mg/L (2)	Conc. Absorbed on zeolite mM/kg (2)
0	0.493	142.65	0.00
1	0.447	124.09	2.48
2	0.45	125.36	2.31
5	0.436	120.54	2.95
15	0.443	122.84	2.64
30	0.432	119.12	3.14
60	0.439	121.62	2.81
120	0.452	126.17	2.20
240	0.444	123.20	2.60
1320	0.456	127.74	1.99
1440	0.448	124.66	2.40

Table C.9. Kinetics batch experiment data for pH 9 and ionic strength 20mM for sample set 1. Final concentration of arsenate was calculated from calibration curve data from AAS.

Sample Set 1 Kinetics pH 9, ionic stength 20mM			
Time (min)	Abs. (1)	Final Conc. mg/L (1)	Conc. Absorbed on zeolite mM/kg (1)
0	0.501	139.17	0.00
1	0.461	123.09	2.15
2	0.451	119.90	2.57
5	0.437	115.28	3.19
15	0.456	121.42	2.37
30	0.438	115.67	3.14
60	0.442	117.01	2.96
120	0.438	115.62	3.14
240	0.438	115.52	3.16
1320	0.442	116.91	2.97
1440	0.447	118.70	2.73

Table C.10. Kinetics batch experiment data for pH 9 and ionic strength 20mM for sample set 2. Final concentration of arsenate was calculated from calibration curve data from AAS.

Sample Set 2 Kinetics pH 9, ionic stength 20mM			
Time (min)	Abs. (2)	Final Conc. mg/L (2)	Conc. Absorbed on zeolite mM/kg (2)
0	0.5	138.62	0.00
1	0.463	123.79	1.98
2	0.454	120.74	2.39
5	0.449	119.12	2.60
15	0.462	123.44	2.03
30	0.435	114.58	3.21
60	0.446	118.14	2.73
120	0.443	117.36	2.84
240	0.439	115.94	3.03
1320	0.449	118.37	2.70
1440	0.446	118.37	2.70

APPENDIX D

BATCH EXPERIMENT DATA FOR ARSENIC AT DIFFERENT pH AND IONIC STRENGTH CONDITIONS

Table D.1. Batch experiment data for pH 4 and ionic strength 1mM for sample set 1. Final concentration of arsenate was calculated from calibration curve data from AAS.

Sample Set 1 Batch experiments pH 4, ionic stength 1mM				
Original Conc. (mg/L)	Abs. (1)	Final Conc. mg/L (1)	Aqueous Conc mM (1)	Conc. Absorbed on zeolite mM/kg (1)
0	0	0.000	0.000	0.000
5	0.001	0.019	0.000	0.665
10	0.002	0.480	0.006	1.271
25	0.016	3.636	0.049	2.852
50	0.06	12.417	0.166	5.016
100	0.21	45.247	0.604	7.308
150	0.373	88.866	1.186	8.160
200	0.495	129.632	1.730	9.392
300	0.195	213.150	2.845	11.592
500	0.354	424.200	5.662	10.117
750	0.505	663.050	8.850	11.606

Table D.2. Batch experiment data for pH 4 and ionic strength 1mM for sample set 2. Final concentration of arsenate was calculated from calibration curve data from AAS.

Sample Set 2 Batch experiments pH 4, ionic stength 1mM				
Original Conc. (mg/L)	Abs. (2)	Final Conc. mg/L (2)	Aqueous Conc mM (2)	Conc. Absorbed on zeolite mM/kg (2)
0	0	0.000	0.000	0.000
5	0.001	0.012	0.000	0.666
10	0.001	0.284	0.004	1.297
25	0.015	3.499	0.047	2.870
50	0.063	13.103	0.175	4.925
100	0.222	48.167	0.643	6.918
150	0.382	91.532	1.222	7.804
200	0.51	135.926	1.814	8.552
300	0.2	219.100	2.924	10.798
500	0.347	412.800	5.510	11.639
750	0.509	672.300	8.974	10.371

Table D.3. Batch experiment data for pH 4 and ionic strength 5mM for sample set 1. Final concentration of arsenate was calculated from calibration curve data from AAS.

Sample Set 1 Batch experiments pH 4, ionic stength 5mM				
Original Conc. (mg/L)	Abs. (1)	Final Conc. mg/L (1)	Aqueous Conc mM (1)	Conc. Absorbed on zeolite mM/kg (1)
0	0	0.000	0.000	0.000
5	0.002	0.529	0.007	0.597
10	0.007	1.646	0.022	1.115
25	0.034	7.301	0.097	2.362
50	0.097	20.923	0.279	3.881
100	0.234	53.136	0.709	6.255
150	0.39	101.763	1.358	6.438
200	0.501	140.904	1.881	7.888
300	0.198	225.700	3.013	9.917
500	0.328	413.100	5.514	11.599
750	0.46	636.200	8.492	15.190

Table D.4. Batch experiment data for pH 4 and ionic strength 5mM for sample set 2. Final concentration of arsenate was calculated from calibration curve data from AAS.

Sample Set 2 Batch experiments pH 4, ionic stength 5mM				
Original Conc. (mg/L)	Abs. (2)	Final Conc. mg/L (2)	Aqueous Conc mM (2)	Conc. Absorbed on zeolite mM/kg (2)
0	0	0.000	0.000	0.000
5	0.003	0.647	0.009	0.581
10	0.008	1.862	0.025	1.086
25	0.033	7.154	0.095	2.382
50	0.098	21.217	0.283	3.842
100	0.24	54.782	0.731	6.036
150	0.387	101.067	1.349	6.531
200	0.501	140.689	1.878	7.917
300	0.201	229.200	3.059	9.450
500	0.326	408.500	5.452	12.213
750	0.462	640.200	8.545	14.656

Table D.5. Batch experiment data for pH 4 and ionic strength 20mM for sample set 1. Final concentration of arsenate was calculated from calibration curve data from AAS.

Sample Set 1 Batch experiments pH 4, ionic stength 20mM				
Original Conc. (mg/L)	Abs. (1)	Final Conc. mg/L (1)	Aqueous Conc mM (1)	Conc. Absorbed on zeolite mM/kg (1)
0	0	0.000	0.000	0.000
5	0.01	2.031	0.027	0.396
10	0.024	4.704	0.063	0.707
25	0.082	16.194	0.216	1.175
50	0.167	34.990	0.467	2.003
100	0.343	79.796	1.065	2.697
150	0.495	129.020	1.722	2.800
200	0.594	170.235	2.272	3.973
300	0.124	267.950	3.576	4.278
500	0.385	457.050	6.101	5.733
750	0.525	691.600	9.231	7.795

Table D.6. Batch experiment data for pH 4 and ionic strength 20mM for sample set 2. Final concentration of arsenate was calculated from calibration curve data from AAS.

Sample Set 2 Batch experiments pH 4, ionic stength 20mM				
Original Conc. (mg/L)	Abs. (2)	Final Conc. mg/L (2)	Aqueous Conc mM (2)	Conc. Absorbed on zeolite mM/kg (2)
0	0	0.000	0.000	0.000
5	0.009	1.847	0.025	0.421
10	0.025	4.827	0.064	0.691
25	0.081	15.959	0.213	1.207
50	0.17	35.714	0.477	1.907
100	0.345	80.398	1.073	2.616
150	0.494	128.633	1.717	2.852
200	0.587	167.459	2.235	4.343
300	0.123	265.500	3.544	4.605
500	0.386	457.550	6.107	5.666
750	0.528	699.500	9.337	6.741

Table D.7. Batch experiment data for pH 7 and ionic strength 1mM for sample set 1. Final concentration of arsenate was calculated from calibration curve data from AAS.

Sample Set 1 Batch experiments pH 7, ionic stength 1mM				
Original Conc. (mg/L)	Abs. (1)	Final Conc. mg/L (1)	Aqueous Conc mM (1)	Conc. Absorbed on zeolite mM/kg (1)
0	0	0.000	0.000	0.000
5	-0.001	0.020	0.000	0.665
10	0.003	0.939	0.013	1.209
25	0.017	3.949	0.053	2.810
50	0.054	14.755	0.197	4.704
100	0.176	49.449	0.660	6.747
150	0.385	96.847	1.293	7.095
200	0.514	139.031	1.856	8.138
300	0.206	232.200	3.099	9.050
500	0.355	429.950	5.739	9.350
750	0.503	661.050	8.823	11.873

Table D.8. Batch experiment data for pH 7 and ionic strength 1mM for sample set 2. Final concentration of arsenate was calculated from calibration curve data from AAS.

Sample Set 2 Batch experiments pH 7, ionic stength 1mM				
Original Conc. (mg/L)	Abs. (2)	Final Conc. mg/L (2)	Aqueous Conc mM (2)	Conc. Absorbed on zeolite mM/kg (2)
0	0	0.000	0.000	0.000
5	-0.001	0.122	0.002	0.651
10	0.002	0.612	0.008	1.253
25	0.014	3.306	0.044	2.896
50	0.058	16.000	0.214	4.538
100	0.177	49.765	0.664	6.705
150	0.381	95.745	1.278	7.242
200	0.502	134.449	1.795	8.749
300	0.2	225.050	3.004	10.004
500	0.36	432.000	5.766	9.076
750	0.513	679.250	9.066	9.443

Table D.9. Batch experiment data for pH 7 and ionic strength 5mM for sample set 1. Final concentration of arsenate was calculated from calibration curve data from AAS.

Sample Set 1 Batch experiments pH 7, ionic stength 5mM				
Original Conc. (mg/L)	Abs. (1)	Final Conc. mg/L (1)	Aqueous Conc mM (1)	Conc. Absorbed on zeolite mM/kg (1)
0	0	0.000	0.000	0.000
5	0.002	0.304	0.004	0.627
10	0.008	1.617	0.022	1.119
25	0.036	7.556	0.101	2.328
50	0.092	20.952	0.280	3.877
75	0.174	41.238	0.550	4.506
100	0.235	57.222	0.764	5.710
125	0.31	78.008	1.041	6.272
150	0.376	98.461	1.314	6.879
200	0.491	139.581	1.863	8.064
300	0.201	229.750	3.067	9.377
500	0.337	427.300	5.703	9.704

Table D.10. Batch experiment data for pH 7 and ionic strength 5mM for sample set 2. Final concentration of arsenate was calculated from calibration curve data from AAS.

Sample Set 2 Batch experiments pH 7, ionic stength 5mM				
Original Conc. (mg/L)	Abs. (2)	Final Conc. mg/L (2)	Aqueous Conc mM (2)	Conc. Absorbed on zeolite mM/kg (2)
0	0	0.000	0.000	0.000
5	0.002	0.323	0.004	0.624
10	0.008	1.529	0.020	1.131
25	0.036	7.468	0.100	2.340
50	0.095	21.727	0.290	3.774
75	0.176	41.817	0.558	4.429
100	0.246	59.976	0.801	5.342
125	0.301	75.480	1.007	6.610
150	0.388	102.096	1.363	6.394
200	0.506	145.599	1.943	7.261
300	0.204	233.600	3.118	8.863
500	0.34	433.650	5.788	8.856
750	0.481	677.750	9.046	9.644

Table D.11. Batch experiment data for pH 7 and ionic strength 20mM for sample set 1. Final concentration of arsenate was calculated from calibration curve data from AAS.

Sample Set 1 Batch experiments pH 7, ionic stength 20mM				
Original Conc. (mg/L)	Abs. (1)	Final Conc. mg/L (1)	Aqueous Conc mM (1)	Conc. Absorbed on zeolite mM/kg (1)
0	0	0.000	0.000	0.000
5	0.01	2.031	0.027	0.396
10	0.024	4.704	0.063	0.707
25	0.082	16.194	0.216	1.175
50	0.167	34.990	0.467	2.003
100	0.343	79.796	1.065	2.697
150	0.495	129.020	1.722	2.800
200	0.594	170.235	2.272	3.973
300	0.124	267.950	3.576	4.278
500	0.385	457.050	6.101	5.733
750	0.525	691.600	9.231	7.795

Table D.12. Batch experiment data for pH 7 and ionic strength 5mM for sample set 1. Final concentration of arsenate was calculated from calibration curve data from AAS.

Sample Set 2 Batch experiments pH 7, ionic stength 20mM				
Original Conc. (mg/L)	Abs. (2)	Final Conc. mg/L (2)	Aqueous Conc mM (2)	Conc. Absorbed on zeolite mM/kg (2)
0	0	0.000	0.000	0.000
5	0.009	1.847	0.025	0.421
10	0.025	4.827	0.064	0.691
25	0.081	15.959	0.213	1.207
50	0.17	35.714	0.477	1.907
100	0.345	80.398	1.073	2.616
150	0.494	128.633	1.717	2.852
200	0.587	167.459	2.235	4.343
300	0.123	265.500	3.544	4.605
500	0.386	457.550	6.107	5.666
750	0.528	699.500	9.337	6.741

Table D.13. Batch experiment data for pH 9 and ionic strength 1mM for sample set 1. Final concentration of arsenate was calculated from calibration curve data from AAS.

Sample Set 1 Batch experiments pH 9, ionic stength 1mM				
Original Conc. (mg/L)	Abs. (1)	Final Conc. mg/L (1)	Aqueous Conc mM (1)	Conc. Absorbed on zeolite mM/kg (1)
0	0	0.000	0.000	0.000
5	0.001	0.017	0.000	0.665
10	0.002	0.500	0.007	1.268
25	0.015	3.450	0.046	2.876
50	0.06	13.749	0.184	4.839
100	0.194	47.951	0.640	6.947
150	0.344	90.523	1.208	7.939
200	0.473	133.025	1.776	8.940
300	0.183	228.900	3.055	9.490
500	0.314	414.700	5.535	11.385
750	0.467	666.900	8.901	11.092

Table D.14. Batch experiment data for pH 9 and ionic strength 1mM for sample set 2. Final concentration of arsenate was calculated from calibration curve data from AAS.

Sample Set 2 Batch experiments pH 9, ionic stength 1mM				
Original Conc. (mg/L)	Abs. (2)	Final Conc. mg/L (2)	Aqueous Conc mM (2)	Conc. Absorbed on zeolite mM/kg (2)
0	0	0.000	0.000	0.000
5	0.001	0.020	0.000	0.665
10	0.001	0.461	0.006	1.273
25	0.015	3.508	0.047	2.869
50	0.055	12.554	0.168	4.998
100	0.196	48.471	0.647	6.878
150	0.332	86.730	1.158	8.445
200	0.459	127.635	1.704	9.659
300	0.185	231.050	3.084	9.203
500	0.32	423.350	5.651	10.231
750	0.457	648.650	8.658	13.528

Table D.15. Batch experiment data for pH 9 and ionic strength 5mM for sample set 1. Final concentration of arsenate was calculated from calibration curve data from AAS.

Sample Set 1 Batch experiments pH 9, ionic stength 5mM				
Original Conc. (mg/L)	Abs. (1)	Final Conc. mg/L (1)	Aqueous Conc mM (1)	Conc. Absorbed on zeolite mM/kg (1)
0	0	0.000	0.000	0.000
5	0.001	0.592	0.008	0.588
10	0.003	1.102	0.015	1.188
25	0.022	7.765	0.104	2.300
50	0.057	20.980	0.280	3.874
100	0.154	57.796	0.771	5.633
150	0.254	100.306	1.339	6.633
200	0.351	149.122	1.990	6.791
300	0.124	227.000	3.030	9.744
500	0.217	410.000	5.473	12.013
750	0.314	629.500	8.402	16.084

Table D.16. Batch experiment data for pH 9 and ionic strength 5mM for sample set 2. Final concentration of arsenate was calculated from calibration curve data from AAS.

Sample Set 2 Batch experiments pH 9, ionic stength 5mM				
Original Conc. (mg/L)	Abs. (2)	Final Conc. mg/L (2)	Aqueous Conc mM (2)	Conc. Absorbed on zeolite mM/kg (2)
0	0	0.000	0.000	0.000
5	0.001	0.520	0.007	0.598
10	0.004	1.673	0.022	1.111
25	0.02	7.357	0.098	2.355
50	0.061	22.418	0.299	3.681
100	0.159	59.827	0.799	5.362
150	0.253	99.684	1.331	6.716
200	0.336	140.673	1.878	7.919
300	0.128	234.100	3.125	8.796
500	0.22	417.150	5.568	11.058
750	0.327	663.650	8.858	11.526

Table D.17. Batch experiment data for pH 9 and ionic strength 20mM for sample set 1. Final concentration of arsenate was calculated from calibration curve data from AAS.

Sample Set 1 Batch experiments pH 9, ionic stength 20mM				
Original Conc. (mg/L)	Abs. (1)	Final Conc. mg/L (1)	Aqueous Conc mM (1)	Conc. Absorbed on zeolite mM/kg (1)
0	0	0.000	0.000	0.000
5	0.009	1.867	0.025	0.418
10	0.025	5.133	0.069	0.650
25	0.076	15.816	0.211	1.226
50	0.169	36.378	0.486	1.818
100	0.338	80.000	1.068	2.670
150	0.497	131.112	1.750	2.521
200	0.596	172.582	2.304	3.660
300	0.237	261.900	3.496	5.085
500	0.381	456.150	6.088	5.853
750	0.524	699.300	9.334	6.767

Table D.18. Batch experiment data for pH 9 and ionic strength 20mM for sample set 2. Final concentration of arsenate was calculated from calibration curve data from AAS.

Sample Set 2 Batch experiments pH 9, ionic stength 20mM				
Original Conc. (mg/L)	Abs. (2)	Final Conc. mg/L (2)	Aqueous Conc mM (2)	Conc. Absorbed on zeolite mM/kg (2)
0	0	0.000	0.000	0.000
5	0.008	1.745	0.023	0.434
10	0.025	5.143	0.069	0.648
25	0.08	16.673	0.223	1.111
50	0.167	36.051	0.481	1.862
100	0.342	81.224	1.084	2.506
150	0.491	128.612	1.717	2.855
200	0.598	173.143	2.311	3.585
300	0.239	264.450	3.530	4.745
500	0.381	455.650	6.082	5.920
750	0.53	711.000	9.490	5.206